

 Open access • Posted Content • DOI:10.1101/2020.11.01.363788

Discovery of five HIV nucleoside analog reverse-transcriptase inhibitors (NRTIs) as potent inhibitors against the RNA-dependent RNA polymerase (RdRp) of SARS-CoV and 2019-nCoV — [Source link](#)

Jialei Sun

Institutions: Discovery Institute

Published on: 01 Nov 2020 - bioRxiv (Cold Spring Harbor Laboratory)

Topics: RNA-dependent RNA polymerase, Polymerase, RNA, Reverse transcriptase and RNA polymerase

Related papers:

- [Comparative Antiviral Activity of Remdesivir and Anti-HIV Nucleoside Analogs Against Human Coronavirus 229E \(HCoV-229E\).](#)
- [Triphosphates of the Two Components in DESCOVY and TRUVADA are Inhibitors of the SARS-CoV-2 Polymerase](#)
- [Specific inhibition of the reverse transcriptase of human immunodeficiency virus type 1 and the chimeric enzymes of human immunodeficiency virus type 1 and type 2 by nonnucleoside inhibitors.](#)
- [HIV-1 reverse transcriptase inhibitors.](#)
- [New developments in anti-HIV chemotherapy.](#)

Share this paper:    

View more about this paper here: <https://typeset.io/papers/discovery-of-five-hiv-nucleoside-analog-reverse-5ava1mwt0b>

1 **Discovery of five HIV nucleoside analog reverse-transcriptase inhibitors (NRTIs)**
2 **as potent inhibitors against the RNA-dependent RNA polymerase (RdRp) of**
3 **SARS-CoV and 2019-nCoV**

4
5 Jialei Sun ^{1,*}

6
7 ¹ Global Health Drug Discovery Institute, Unit B, Block 2, Zhongguancun Dongsheng
8 International Science Park, 1 Yongtaizhuang North Road, Haidian District, Beijing,
9 China 100192

10
11 * Correspondence: jialei.sun@ghddi.org

12
13 **Abstract**

14 The outbreak of SARS in 2002-2003 caused by SARS-CoV, and the pandemic of
15 COVID-19 in 2020 caused by 2019-nCoV (SARS-CoV-2), have threatened human
16 health globally and raised the urgency to develop effective antivirals against the viruses.
17 In this study, we expressed and purified the RNA-dependent RNA polymerase (RdRp)
18 nsp12 of SARS-CoV and developed a primer extension assay for the evaluation of
19 nsp12 activity. We found that nsp12 could efficiently extend single-stranded RNA, while
20 having low activity towards double-stranded RNA. Nsp12 required a catalytic metal
21 (Mg^{2+} or Mn^{2+}) for polymerase activity and the activity was also K^{+} -dependent, while
22 Na^{+} promoted pyrophosphorylation, the reverse process of polymerization. To identify
23 antivirals against nsp12, a competitive assay was developed containing 4 natural
24 rNTPs and a nucleotide analog, and the inhibitory effects of 24 FDA-approved
25 nucleotide analogs were evaluated in their corresponding active triphosphate forms.
26 Ten of the analogs, including 2 HIV NRTIs, could inhibit the RNA extension of nsp12
27 by more than 40%. The 10 hits were verified which showed dose-dependent inhibition.
28 In addition, the 24 nucleotide analogs were screened on SARS-CoV primase nsp8
29 which revealed stavudine and remdesivir were specific inhibitors to nsp12.
30 Furthermore, the 2 HIV NRTIs were evaluated on 2019-nCoV nsp12 which showed

31 inhibition as well. Then we expanded the evaluation to all 8 FDA-approved HIV NRTIs
32 and discovered 5 of them, tenofovir, stavudine, abacavir, zidovudine and zalcitabine,
33 could inhibit the RNA extension by nsp12 of SARS-CoV and 2019-nCoV. In conclusion,
34 5 FDA-approved HIV NRTIs inhibited the RNA extension by nsp12 and were promising
35 candidates for the treatment of SARS and COVID-19.

36

37 **Introduction**

38 Severe acute respiratory syndrome coronavirus (SARS-CoV) and 2019-nCoV (SARS-
39 CoV-2) belong to *Betacoronavirus* genus, *Coronaviridae* family and they have a single-
40 stranded, positive-sense RNA genome which is approximately 30kb [1, 2]. SARS-CoV
41 originates from bat and is transmitted to human through an intermediate host, palm
42 civet [3, 4]. 2019-nCoV is also widely accepted to have a bat origin as it is highly similar
43 to a bat coronavirus RaTG13 throughout the genome with 96.2% identity [5]. The high
44 identity suggests a close relationship between the two viruses and there is no
45 recombination event for both of them after they separated from each other evolutionally
46 [4]. However, it is still unclear whether and when an intermediate host have been
47 involved in the zoonotic transmission to human. Soon after the outbreak, pangolin was
48 proposed to be the intermediate host when a pangolin-CoV was discovered which
49 shared 91.02% identity with 2019-nCoV on whole genome level [6, 7]. The discovery
50 provides evidence for the presence of an intermediate host, but 91.02% identity is still
51 too low to suggest a direct transfer from the pangolin to human. Recently, it is reported
52 that ACE2 from multiple animals can bind the spike protein of 2019-nCoV and support
53 infection [8, 9], especially the ACE2 from monkeys which is identical to and binds as
54 efficient as human [8, 10]. These studies also provides evidence for the involvement
55 of an intermediate host. In addition, studies have revealed that 2019-nCoV has been
56 under different types of natural selection. Its genome contains uncommon high ratio of
57 neutral mutations which are featured by the predominance of C-U substitution [11-13].
58 The neutral mutations suggested there was strong selection pressure on 2019-nCoV
59 and raised the possibility of that the virus stayed in a single type of host, possibly bat,
60 for a very long period. The spike of 2019-nCoV appears to have been optimized for

61 the binding to human ACE2 with a 1000-fold higher binding affinity than its closest
62 relative, RaTG13 [14, 15]. And the spike also has acquired a polybasic furin cleavage
63 site which is essential for its entry into host cell [16, 17]. These studies reveal strong
64 purifying selection on the spike region of 2019-nCoV [18, 19], suggesting the
65 adaptation from its original host to human is a rapid process. To explain the natural
66 selection on 2019-nCoV, several hypotheses have been proposed, including selection
67 in an animal host before zoonotic transfer, selection in humans following zoonotic
68 transfer and selection during passage [14]. To better understand the origin of the virus,
69 more studies are required.

70

71 For antiviral development, currently, there are at least three promising viral drug targets:
72 spike protein (S), main protease (Mpro)/3C-like protease (3CLpro), and RNA-
73 dependent RNA polymerase (RdRp). The spike of SARS-CoVs is a trimer and has two
74 subunits, S1 and S2. The binding to its human receptor angiotensin-converting enzyme
75 2 (ACE2) is mediated by the receptor binding domain (RBD) located in the S1 subunit
76 [20-23]. Upon binding to ACE2, spike undergoes conformational change to facilitate
77 the fusion between viral membrane and host cell membrane [24]. The binding affinity
78 between 2019-nCoV spike and ACE2 was reported to be 10-fold and 1000-fold higher
79 than the spikes of SARS-CoV and its closest known relative RaTG13, respectively [15,
80 21]. High receptor binding affinity must have enhanced the human-to-human
81 transmission of 2019-nCoV. As an essential factor for the infectivity of SARS-CoVs and
82 the main target of neutralizing antibodies upon infection, spike has been a major drug
83 target for antiviral discoveries, including neutralizing antibodies development such as
84 LY-CoV555 and JS016 [25-30], inhibitor development [31] and vaccines [32-36].
85 According to Covid-19vaccinetracker.org, by September 2020, 35 vaccines in total
86 were under different stages of clinical trials for COVID-19 and 10 of them were 2019-
87 nCoV spike or spike subunit-based [37].

88

89 The main protease of SARS-CoVs, Mpro, also called 3CLpro, is encoded by nsp5
90 region. It is the major enzyme for polyprotein cleavage to produce mature and

91 functional viral proteins [38]. Due to its essential role for SARS-CoVs, Mpro has been
92 an attractive target for antiviral drug discoveries [39]. It is a cysteine protease and
93 needs to form homodimer to be active [40-43]. The substrate residues at the cleavage
94 site are conservative [44]. Currently, there are at least three drug discovery strategies
95 for Mpro: structure-based drug design, biochemical assay screening and virtual
96 screening. Since the outbreak of COVID-19, intense efforts have been made on virtual
97 screening and multiple drugs have been predicted to be effective [45-50]. Drugs
98 targeting Mpro are usually classified into two subgroups: peptidomimetics and small
99 molecules [51]. Lopinavir/ritonavir (LPV/r), repurposed from HIV protease inhibitors,
100 belongs to the peptidomimetics group. Although LPV/r was predicted to be potent
101 initially, no benefit was reported after it was systematically investigated for the
102 treatment of COVID-19 in clinical trials [52-57],

103

104 SARS-CoVs have two RNA-dependent RNA polymerases (RdRp): nsp12 and nsp8.
105 Nsp12 is the main RdRp and plays the major role in the replication of RNA genome
106 [58, 59]. Nsp8 is a non-canonical, sequence-specific RdRp and proposed to be the
107 primase for SARS-CoVs [60, 61]. To replicate long RNA, nsp12 needs to interact with
108 nsp7 and nsp8 to form a stable replication complex [62, 63]. Like all viral RdRps, nsp12
109 is right hand-shaped and composed of a fingers domain, a palm domain and a thumb
110 domain [62]. The RNA polymerase activity is mediated by seven conserved motifs (A
111 to G) [64, 65]. In addition, distinguished from most viruses, the nsp12 of SARS-CoVs
112 also contains a nidovirus-unique N-terminal extension domain (NiRAN) which can
113 covalently bind guanosine and uridine and has nucleotidylation activity [66]. The
114 function of NiRAN in RNA replication is still unclear. As an attractive target for antiviral
115 discoveries, efforts have been made on nsp12 since the outbreak of COVID-19, which
116 mainly focus on drug-repurposing of FDA-approved drugs, especially on nucleotide
117 analogs. Approaches for the repurposing include virtual screening, *in vitro* biochemical
118 assays and cell culture-based assays [67, 68]. Virtual screening usually focuses on the
119 binding between nsp12 and a compound, although interfering the interface between
120 nsp12 and nsp8 or nsp7 has also been investigated [69, 70]. Hundreds of hits have

121 been yielded by virtual screening, such as remdesivir, ribavirin, galidesivir, tenofovir,
122 IDX-184 [71], and sofosbuvir [71-73]. Biochemical assays take advantage of purified
123 proteins, mostly nsp12/nsp7/nsp8 replication complex, and have also identified useful
124 antiviral nucleotide analogs against 2019-nCoV, including sofosbuvir, alovudine,
125 zidovudine, tenofovir, abacavir, lamivudine, emtricitabine, cidofovir,
126 valganciclovir/ganciclovir, stavudine and entecavir [72, 74-77]. These nucleotide
127 analogs could be incorporated into extending RNA and terminate further chain
128 elongation. Cell culture-based assays involve infectious live viruses and are the most
129 direct approach to identify antivirals among the three. Studies using this approach have
130 identified ribavirin, remdesivir, gemcitabine, and tenofovir in disoproxil fumarate form
131 (TDF) to be inhibitors for SARS-CoVs [78-82]. Among them, ribavirin and remdesivir
132 have been evaluated in clinical trials [83, 84] and remdesivir has been approved by
133 FDA recently as it can shorten the time to recovery for patients.

134

135 In this study, we would focus on drug-repurposing of FDA-approved nucleotide analogs
136 using a novel biochemical assay. And we managed to use nsp12 itself, instead of
137 nsp12/nsp7/nsp8 complex, as the sole target for antiviral discovery. The nsp12 of
138 SARS-CoVs was expressed and purified and its RNA extension activity was
139 characterized under various conditions, especially its dependence on K^+ and Mg^{2+} .
140 Furthermore, we developed a competitive assay which was able to quantify the relative
141 inhibition abilities among nucleotide analogs, instead of using previously reported
142 chain termination assays which could only give qualitative identification whether a
143 nucleotide analog was a chain terminator for nsp12. Using the competitive assay, we
144 identified 10 nucleotide analogs with >40% inhibition on SARS-CoV nsp12. Two of the
145 hits were HIV NRTIs. We further evaluated all 8 FDA-approved HIV NRTIs and
146 discovered 5 of them could inhibit the nsp12 of SARS-CoV and 2019-nCoV.

147

148 **Materials and Methods**

149 **Chemicals**

150 6-Mercaptopurine-TP (NU-1110S), 6-chloropurine-TP (NU-1109S), clofarabine-TP

151 (NU-874), 6-methylthio-GTP (NU-1130S), 6-thio-GTP (NU-1106S), stavudine-TP (NU-
152 1604S), 8-oxo-GTP (NU-1116S), gemcitabine-TP (NU-1607S), acyclovir-TP (NU-877),
153 ganciclovir-TP (NU-275S), lamivudine-TP (NU-1606L) and zidovudine-TP (NU-989S)
154 were purchased from Jena Bioscience. Tenofovir-DP (FT44596), 2'-C-M-GTP
155 (NM08170), 2'-C-M-CTP (NM29280), emtricitabine-TP (ME16706) and gemcitabine-
156 TP (ND09708) were purchased from Carbosynth. 2'-O-methyl-UTP (N-1018), 2'-azido-
157 2'-dUTP (N-1029), 2'-amino-2'-dUTP (N-1027), ara-UTP (N-1034), 3'-O-methyl-UTP
158 (N-1059), 2'-F-2'-dUTP (N-1010-1) and didanosine-TP (N-4017-1) were purchased
159 from Trilink. Remdesivir-DP was synthesized by WuXi AppTech. Sofosbuvir-DP (HY-
160 15745) was purchased from MedChemExpress. Ribavirin-TP (sc-358826) was
161 purchased from Santa Cruz Biotechnology. Zalcitabine-TP (Z140050) and abacavir-
162 TP/carbovir-TP (C177755) were purchased from TRC Canada.

163

164 **RNA primer-template annealing**

165 RNA primer and templates were synthesized by Genscript. The sequences were
166 modified from a previous study [85] and designed to be non-secondary structure
167 forming. To form an RNA primer-template (P/T) complex, the primer (Cy5.5-5'-
168 AACGUCUGUUCGCAAAAAGC-3') was mixed with a template (5'-
169 CUUAUUCGAGCUUUUUGCGAACAGACGUU-3') in a ratio of 1:3 in 50 mM NaCl. The
170 mixture was heated up to 95°C and slowly cooled down to 25°C by a PCR machine.
171 The program was: 95°C for 5 min, 2°C decrease/10 s for 23 cycles, 51°C for 5 min,
172 2°C decrease/20 s for 14 cycles. The RNA primer was annealed to a stem-loop
173 forming template (5'- CUAUUGACUUGCUUUUUCGCUACAGACGUU-3') by the
174 same procedure.

175

176 **Template-dependent RNA primer extension assay**

177 Nsp12 template-dependent primer extension activity was determined by annealed
178 RNA primer-template (P/T) complex. The assay condition contained 25 mM Tris HCl
179 pH 8.0, 50 mM KCl or NaCl, 1 mM DTT, various concentrations of MgCl₂ or MnCl₂, 10
180 nM P/T complex, 32 nM purified nsp12 and 100 μM rNTPs (25 μM each). 10% Glycerol,

181 5 mM NaCl and 0.02% triton X-100 were introduced by nsp12 stock. Extra 1 mM NaCl
182 was introduced by P/T complex which was prepared in 50 mM NaCl. The reaction was
183 performed in 25 μ l system and incubated at 37°C for 2 h. Poly A assay was performed
184 in a similar condition containing 25 mM Tris HCl pH 8.0, 50 mM KCl or NaCl, 1 mM
185 DTT, 0.5 mM MgCl₂, 10 nM P/T complex, 16 nM nsp12 and 250 μ M either ATP, UTP,
186 GTP or CTP or a combination. Water was used as control. Combination assay of nsp12,
187 nsp7 and nsp8 was also performed in a similar condition: 25 mM Tris HCl pH 8.0, 1
188 mM DTT, 0.5 mM MgCl₂, 10 nM P/T complex, 100 μ M rNTPs and 50 mM KCl.
189 Concentrations of nsp12, nsp7 and nsp8 were 16 nM, 400 nM and 400 nM, respectively.
190 Reaction was quenched by adding 50 μ l quenching buffer which contained 90 mM Tris
191 base, 29 mM taurine, 10 mM EDTA, 8 M urea, 0.02% SDS and 0.1% bromophenol
192 blue. The reaction was then denatured at 95°C for 20 min, analyzed by 15% denaturing
193 polyacrylamide urea gel electrophoresis and visualized using an Odyssey scanner (LI-
194 COR).

195

196 **Combinational assay of nsp12 and helicase nsp13**

197 The assay condition contained 25 mM Tris HCl pH 8.0, 50 mM KCl, 1 mM DTT, 1 mM
198 MgCl₂, 10 nM P/T complex, 16 nM nsp12, 210 or 420 nM nsp13, and 100 μ M rNTPs
199 (25 μ M each). 10% Glycerol, 5 mM NaCl and 0.02% triton X-100 were introduced by
200 nsp12 and nsp13 stocks. Extra 1 mM NaCl was introduced by P/T complex stock. The
201 reaction was performed in 25 μ l system and incubated at 37°C for 2 h. Activity on
202 single-stranded RNA in the assay was performed with 10 nM the RNA primer instead
203 of P/T complex. The concentrations of nsp12, nsp13, nsp7 and nsp8 were 16 nM, 420
204 nM, 6.25 μ M and 1.25 μ M, respectively.

205

206 **Back-priming extension assay**

207 The activity of nsp12 in this assay was determined by the synthesized Cy5.5-labeled
208 single-stranded RNA primer without a template. The assay condition contained 25 mM
209 Tris HCl pH 8.0, 50 mM KCl, 1 mM DTT, 1 mM MgCl₂, 10 nM RNA primer, 16 nM
210 purified nsp12 and 100 μ M rNTPs (25 μ M each). 5% or 10% glycerol, 2.5 or 5 mM

211 NaCl, and 0.01% or 0.02% triton X-100, were introduced by nsp12 stock, depending
212 on the volume of nsp12 stock added in the system. Extra 1 mM NaCl was introduced
213 by RNA primer stock which was prepared in 50 mM NaCl. The assay was performed
214 in 25 μ l system reaction at 37°C for 30 min, unless otherwise specified.

215

216 **Competitive assay for nsp12 and nsp8 screening**

217 The inhibitory effects of 24 FDA-approved nucleotide analogs against nsp12 and nsp8
218 were determined using the exact back-priming extension assay mentioned above
219 which was performed in 25 μ l system and contained 16 nM purified nsp12 and 100 μ M
220 rNTPs (25 μ M each). Nucleotide analogs were evaluated at 4 mM except for
221 emtricitabine-TP which was evaluated at 2 mM due to low stock concentration. 4 mM
222 ATP, UTP, GTP or CTP were used as controls. Assay with 100 μ M rNTPs only was
223 also included as control. The screening assay for nsp12 was incubated at 37°C for 30
224 min. Nsp8 was screened at 1.25 μ M and incubation period for nsp8 was extended to
225 60 min due to the relatively lower activity of nsp8. Verification of nsp12 hits and hits
226 evaluation on 2019-nCoV nsp12 were performed in the same condition. Reaction
227 system was 25 μ l and 15 μ l, respectively. Extension products were then analyzed by
228 15% denaturing Urea-PAGE gel electrophoresis and scanned by an Odyssey scanner
229 (LI-COR). Extended products were quantified using Image Studio software (LI-COR)
230 and the intensity of ATP, UTP, GTP and CTP products were averaged. Product intensity
231 of nucleotide analogs were then compared to the rNTP average of which the activity
232 was defined as 100%, relative intensity and percent of inhibition were calculated.

233

234 **Concentration optimization of catalytic metals for nsp12 activity**

235 The assay condition contained 25 mM Tris HCl pH 8.0, 50 mM KCl, 1 mM DTT, 10 nM
236 RNA primer, 16 nM nsp12 and 100 μ M rNTPs. The assay also contained 5% glycerol
237 and 0.01% triton X-100 which were introduced by nsp12 stock. 3.5 mM NaCl was
238 introduced by nsp12 stock and RNA primer stock. For catalytic metals optimization,
239 nsp12 activities were determined at various concentrations of MgCl₂ or MnCl₂, from
240 0.0625 to 2 mM. Control was performed with same volume of water. The assay was

241 re-performed with adding 0.5 mM EDTA into the reaction system, to chelate and block
242 the catalytic activity of endogenous metals. For EDTA titration of endogenous metals,
243 nsp12 activity was determined at various EDTA concentrations (1 nM to 100 μ M)
244 without adding MgCl₂ or MnCl₂. Reaction mix was incubated at 37°C for 30 min.

245

246 **Concentration optimization of KCl and NaCl for nsp12 activity**

247 The assay condition contained 25 mM Tris HCl pH 8.0, 1 mM MgCl₂, 1 mM DTT, 10
248 nM Cy5.5-labeled RNA primer, 16 nM nsp12 and 100 μ M rNTPs. The assay also
249 contained 10% glycerol, 0.02% triton X-100 and 6 mM NaCl introduced by nsp12 and
250 Cy5.5-RNA stocks. Nsp12 activity was determined at various concentrations of KCl or
251 NaCl, from 10 to 200 mM, with water used as control. An enzymatic control was
252 performed with 50% glycerol instead of purified nsp12. Reaction mix was incubated at
253 37°C for 30 min.

254

255 **Time-course study of nsp12**

256 The activity of nsp12 was determined in the same condition as back-priming extension
257 assay. The reaction mix was prepared on ice and then incubated at 37°C. At various
258 time-points (5-120 min), reactions were quenched and denatured immediately. The
259 reaction products were then visualized and analyzed. Reaction with 50% glycerol
260 instead purified nsp12 was used as enzymatic control which was incubated at 37°C for
261 120 min.

262

263 **Protein purification**

264 All sequences in this study were synthesized by Genscript and constructed into pMAL-
265 c5x vector with N-MBP and C-6X His tags. The sequences of SARS-CoV nsp12, nsp7
266 and nsp8 were adopted from a previous study [62] and constructed into pMAL-c5x
267 vector between Nde I and EcoR I restriction sites. SARS-CoV nsp13 (nt 16167 to
268 17966, accession no.: NC_004718.3) was constructed into the vector between Nde I
269 and BamH I sites. And 2019-nCoV nsp12 (nt 13468 to 16233, accession no.:
270 NC_045512.2) was constructed between Nde I and Pst I. For protein purification, p-

271 MAL-c5x-nsp12-His was transformed into *E. coli* BL21 (DE3) (Transgen, CD601-02)
272 and protein expression was induced by an auto-induction system (71757-5, EMD
273 Millipore). Upon overnight induction at 25°C, bacterial cell culture was collected and
274 lysed with lysis buffer (20 mM Tris pH 8.0, 500 mM NaCl, 10% glycerol, 0.5% triton X-
275 100, 2 mM MgCl₂, 0.1 mM ZnCl₂, 10 mM DTT, and 0.5X protease inhibitor cocktail, HY-
276 K0010, MCE). Cell lysis was centrifuged at 5000 g for 30 min at 4°C to remove cell
277 debris. Supernant was then applied to amylose resin (E8021L, NEB) for 3-5 h at 4°C
278 to bind MBP-nsp12. Resin was then washed three times with washing buffer (20 mM
279 Tris pH 8.0, 500 mM NaCl, 10% glycerol, 1% triton X-100, 1 mM DTT). To release
280 nsp12 from MBP tag, the resin was treated with factor Xa protease (P8010L, NEB)
281 overnight at 4°C. Supernant was collected and applied to a Ni-NTA resin (88222,
282 Thermo) for 1-2h at 4°C to bind nsp12. The resin was washed three times with washing
283 buffer and nsp12 was eluted with elution buffer (20 mM Tris pH 8.0, 50 mM NaCl, 10%
284 glycerol, 0.1% triton X-100, 1 mM DTT, 300 mM imidazole). The concentration of
285 glycerol was then adjusted to 50% and nsp12 stock was stored at -20°C. Nsp7, nsp8,
286 nsp13 and 2019-nCoV nsp12 was purified by the same procedure. The concentrations
287 of purified proteins were quantified by running an SDS-PAGE and comparing them with
288 serially diluted BSA.

289

290 **Results**

291 **Protein purification of the nsp12 of SARS-CoV and 2019-nCoV**

292 Proteins in this study were expressed in *Escherichia coli* with MBP at N-terminus and
293 6X His at C-terminus. MBP was removed by factor Xa protease to produce His-tagged
294 proteins for downstream assays. To simplify, his tag was omitted from the protein
295 names. **Figure 1A** showed the purified SARS-CoV and 2019-nCoV proteins on SDS-
296 PAGE and the targets to purify were indicated by stars (*). The identities of proteins
297 were confirmed by Mass spectrometry (**Supplementary Table 1**). Production of
298 SARS-CoV nsp12 per liter was low compared to nsp7, nsp8 and nsp13. Nsp12 had a
299 large size (100 KD) which must have affected its correct folding during expression. The
300 bulky size must also have restricted the access of factor Xa protease to its cleavage

301 site which was located between MBP and nsp12, leading to the decrease of cleavage
302 efficiency. These could explain the low production observed for nsp12. The production
303 of 2019-nCoV nsp12 was low as well, which was consistent with SARS-CoV. In
304 addition, as shown in the figure, there were 5 extra protein bands for nsp12 which were
305 **(a)** MBP-nsp12, **(b)** 60 KD chaperone protein GroEL, **(c)** MBP, **(d)** elongation factor Tu,
306 and **(e)** 30S ribosomal protein S3, as identified by Mass. GroEL is a major chaperone
307 for protein folding in *E. coli* [86], it might have bound to nsp12 during expression to
308 promote and maintain the correct folding of nsp12. Production of nsp7, nsp8 and nsp13
309 was relatively abundant and nsp8 showed an alternative product at 10 KD, indicated
310 by **(#)**, which should be due to non-specific cleavage by factor Xa protease. The
311 alternative product was confirmed by Mass as well.

312

313 **SARS-CoV nsp12 had low extension activity on double-stranded RNA**

314 It has been reported that the RNA polymerase activity of SARS-CoV nsp12 is primer
315 dependent [59]. Therefore, upon purification, a Cy5.5-labeled RNA primer was
316 annealed to its RNA template to form an RNA primer-template (P/T) complex and the
317 activity of nsp12 was determined using the P/T complex. The condition for activity
318 determination contained 50 mM KCl or NaCl combined with various concentrations of
319 MgCl₂ or MnCl₂. Active nsp12 would extend the primer and fully extended product
320 would have 9 more nucleotides (nt). As shown by **Figure 1B**, consistent with a previous
321 study, nsp12 only showed activity with distributive product bands in the presence of
322 Mn²⁺, while very low activity was observed for Mg²⁺ [58]. However, as Mg²⁺ had a higher
323 concentration and was the predominant catalytic metal for DNA/RNA polymerases
324 intracellularly [87], we did not continue the study with Mn²⁺ which did not represent the
325 real physiological condition. For Mg²⁺, the activities of nsp12 were evaluated for both
326 K⁺ and Na⁺. Both showed very weak activities with faint bands indicated by red (>). As
327 extension lengths of the bands were close to the predicted 9 nt, we initially thought
328 they were real template-dependent primer extension activities. However, when we
329 further performed studies with ATP only instead of all 4 rNTPs, nsp12 showed same
330 extension products (**Figure S1**). This activity was not detected for UTP, GTP, CTP or

331 their combinations. Therefore, nsp12 could utilize ATP as the sole source for primer
332 extension under the conditions tested and the activities observed for Mg^{2+} was poly A
333 activity, not template-dependent primer extension. To identify the real activity, we then
334 determined the activity of nsp12 in the presence of nsp7 and nsp8 (**Figure 1C**), as
335 nsp12 has been reported to form complex with nsp7 and nsp8 to be active. As
336 compared to nsp12 alone, the combination with nsp7 and nsp8 had similar level of
337 products, suggesting that nsp7 and nsp8 did not significantly enhance the activity of
338 nsp12 in the condition tested. Nsp7, nsp8 and combination of the two were not active
339 completely. Taken together, these results suggested nsp12 had low activities towards
340 the double-stranded RNA.

341

342 **Nsp12 had high activity towards single-stranded RNA**

343 Despite of repeatings under various conditions for months, we were not able to improve
344 the activity with the double-stranded RNA P/T complex, possibly due to the low
345 concentration of nsp12 (16 nM) which was much lower than reported studies [59, 88].
346 Then we noticed that, in the presence of K^+ , there was another weak product band
347 (**Figure 1B**), which was indicated by red star (*). The product had extended 7 nt as
348 compared to the distributive bands catalyzed by Mn^{2+} . As the product was weak and 2
349 nt shorter than fully extended product which was 9 nt, we hypothesized that the activity
350 of nsp12 was hindered by the helix force of double-stranded RNA and it needed to
351 couple with helicase to achieve high activity and long extension. To test , we purified
352 the helicase nsp13 of SARS-CoV (**Figure 1A**) which had been reported to have
353 protein-protein interaction with nsp12 [89-91]. Following the purification, we designed
354 a stem loop-forming P/T complex as well as the P/T complex used above with perfect
355 base-pairings for the determination of nsp12 activity in combination with nsp13 (**Figure**
356 **2A**). The molar ratios of nsp12 and nsp13 in the combination were 1:13 and 1:26.
357 Reaction with 50% glycerol was used as control. As shown by **Figure 2B**, upon
358 combination, the activity of nsp12 was enhanced by nsp13 in a dose-dependent
359 manner. The enhancement was especially obvious for the P/T complexes with stem-
360 loop structure. This result suggested nsp13 did enhance the activity of nsp12. However,

361 extension length of the product was still 7 nt instead of the predicted 9 nt. This
362 observation was against the coupling model between nsp12 and nsp13, as the helix
363 unwinding by nsp13 should lead to longer extension of nsp12. Then, we realized that
364 nsp12 was active towards the single-stranded RNA primer. The enhancement of nsp12
365 activity observed was due to the release of more single-stranded primer by nsp13 from
366 the double-stranded P/T complex. To confirm, the assay was performed with the single-
367 stranded primer without the annealing to a template and almost full activity was
368 observed for nsp12 (**Figure 2B**). This type of activity of nsp12 should be due to the
369 back-priming of RNA primer of which the 3' end bends back and pairs within the primer
370 to form an extendable hairpin structure, which has been reported for nsp12 previously
371 [63, 88]. Taken together, these results showed that nsp12 had high activity towards the
372 single-stranded RNA primer. In addition, nsp8 and nsp7+nsp8 complex also showed
373 high activities which was not surprising as nsp8 was presented to be the primase for
374 SARS-CoVs [60, 92]. Interestingly, nsp13 and nsp7 also showed weak activities which
375 possibly had relationship with their abilities to bind RNA. As shown in **Figure 1B**, the
376 product had 7 nt extension, we analyzed the primer sequence (Cy5.5-5'-
377 AACGUCUGUUCGCAAAAAGC-3') and found that the 5'-AGC-3' at 3'-terminus could
378 form a double parings with 3'-UUG-5' in the sequence. The full extension for this paring
379 was 7 nt (5'-AGACGUU-3') which had 2 A, 2 G, 2 U and 1 C (**Figure 2C**). Therefore,
380 the sequence of the extended product was predicted to be Cy5.5-5'-
381 AACGUCUGUUCGCAAAAAGCAGACGUU -3', which formed a stem-loop structure.

382

383 **Catalytic metals were required for nsp12 activity**

384 To characterize nsp12, we first performed time-course study to analyze the activity of
385 nsp12 at different time-points using the single-stranded RNA primer (**Figure 3A**).
386 Extended product could be observed as early as 5 min, suggesting that the RNA
387 extension by nsp12 was very fast. The product increased in a time-dependent manner
388 with the decrease of primer. At 30 min, significant amount of product could be observed.
389 At 120 min, almost full activity was observed with little primer left. This study confirmed
390 the activity of nsp12 observed in **Figure 2B** and suggested the extension of the single-

391 stranded RNA primer by nsp12 was very efficient.

392

393 DNA or RNA polymerases required a divalent cation, mostly Mg^{2+} , to catalyze DNA or
394 RNA extension. To further characterize nsp12, we determined the dependence of
395 nsp12 on Mg^{2+} and Mn^{2+} (**Figure 3B**). Both Mg^{2+} and Mn^{2+} could catalyze the extension
396 by nsp12 and optimal activities were observed from 62.5 μ M to 1 mM for Mg^{2+} and
397 from 62.5 μ M to 0.25 mM for Mn^{2+} . Intracellular Mg^{2+} concentration is 0.5-1 mM which
398 was within this range [93] and intracellular Mn^{2+} concentration ranges from 10 to 200
399 μ M [94, 95] which was also widely overlapped with the concentrations evaluated. At
400 high concentrations (2 mM), Mg^{2+} and Mn^{2+} started to decrease the activity of nsp12.
401 This result showed that a wide range of concentrations of Mg^{2+} or Mn^{2+} could support
402 the optimal activity for nsp12. To our surprise, the control without adding Mg^{2+} or Mn^{2+}
403 also showed activity, though sub-optimal. This should be due to the endogenous
404 catalytic metals introduced by protein purification buffers or other reagents used in the
405 assay. To prove this hypothesis, we repeated the assay in the presence of 0.5 mM
406 EDTA (**Figure 3C**), which could chelate catalytic metals in 1:1 ratio. As expected,
407 activity of the control without Mg^{2+} or Mn^{2+} was blocked completely. The activities of
408 Mg^{2+} at low concentrations (62.5-250 μ M) were also blocked while optimal activities
409 were observed from 0.5 to 2 mM. For Mn^{2+} , activity was blocked at 62.5 μ M and optimal
410 activity was observed at 1 mM. The activity blocking by EDTA suggested that the
411 activity in the control was due to endogenous catalytic metals and nsp12 did require
412 Mg^{2+} or Mn^{2+} for RNA extension. Furthermore, we performed the assay without adding
413 Mg^{2+} or Mn^{2+} and titrated the concentration of endogenous catalytic metals using
414 serially diluted EDTA (**Figure 3D**). As compared to control without EDTA, activities
415 remained optimal from 1 nM to 10 μ M, suggesting EDTA in the range was insufficient
416 to chelate the metals. However, at 100 μ M, the activity of nsp12 was fully blocked. As
417 EDTA blocked metals in 1:1 ratio, this result suggested that the concentration of
418 endogenous catalytic metals was below 100 μ M. When Mg^{2+} was re-introduced into
419 the assay system, activity was re-observed. Taken together, these results suggested
420 that catalytic metals were required for nsp12 activity and optimal activity could be

421 maintained in a wide range of concentrations of Mg^{2+} or Mn^{2+} , including physiological
422 concentrations.

423

424 **The activity of nsp12 was K^+ -dependent**

425 Although monovalent cations were not catalytic to DNA/RNA polymerases, they did
426 play an important role in maintaining ion strength which was also essential for
427 polymerase to achieve optimal activities [96, 97]. In addition, monovalent cations also
428 affect the stability of RNA tertiary structure [98-100]. To characterize how monovalent
429 cations would affect nsp12, we determined the activity of nsp12 at various
430 concentrations of K^+ and Na^+ (**Figure 3E**). As compared to the enzymatic control which
431 was performed with 50% glycerol instead of nsp12, RNA extension activities were
432 observed for K^+ , but not for Na^+ . The extension activities increased in a dose-
433 dependent manner from 10 to 50 mM and maintained optimal from 50 to 150 mM.
434 Physiological concentration of K^+ was 140-150 mM which was within this range [101].
435 At 200 mM, the activity started to decrease. In contrast, for Na^+ , no extension activity
436 was detected throughout the concentrations evaluated (10 to 200 mM). However,
437 abundant pyrophosphorylation products were observed, indicating that nsp12 was also
438 active in the presence of Na^+ but the activity only led to pyrophosphorylation. In
439 addition, the control without adding K^+ or Na^+ which contained 6 mM NaCl introduced
440 by nsp12 and Cy5.5-RNA stocks, also showed pyrophosphorylation. This result
441 suggested that nsp12 depended on K^+ to have RNA extension activity and optimal
442 activity required high K^+ concentration.

443

444 **Discovery of 10 nucleotide analogs with inhibition against SARS-CoV nsp12**

445 Based on the characterization of nsp12, we then developed a competitive assay for
446 drug screening. The assay contained 25 mM Tris HCl pH 8.0, 50 mM KCl, 1 mM DTT,
447 1 mM $MgCl_2$, 16 nM nsp12, 10 nM single-stranded RNA primer, 100 μ M rNTPs (25 μ M
448 each) and a nucleotide analog. The analog would compete with its corresponding rNTP,
449 either ATP, UTP, GTP or CTP, and inhibit the RNA extension by nsp12. We collected a
450 small drug library which contained 24 nucleotide analogs, mostly FDA-approved,

451 including two gemcitabine from different suppliers. The analogs were all in their
452 corresponding triphosphate forms to be active in biochemical assays. But to simplify,
453 they were represented by their common drug names instead of triphosphates, unless
454 otherwise specified. Initially, 12 of the analogs were tested as a trial and we found 2'-
455 C-M-GTP could inhibit the RNA extension by nsp12 at 2 mM (**data not shown**). To
456 optimize the concentration for screening, we then performed dose-response study for
457 2'-C-M-GTP (**Figure 4A**). Control was added with 100 μ M rNTPs and same amount of
458 water. From 0.25 to 1 mM, 2'-C-M-GTP showed similar levels of product to the control,
459 suggesting it did not inhibit nsp12 at these concentrations. At 2 mM, inhibition could be
460 observed as shown by the decrease of product. And at 4 mM, nearly full inhibition was
461 observed. Inhibition on pyrophosphorylation was also observed for 2'-C-M-GTP at 4
462 mM. Remdesivir at 2 mM was not effective. This assay showed less products with full
463 extension instead of similar amount of products with shorter extension. This type of
464 inhibition was surprising as nucleotide analogs were supposed to be incorporated into
465 extending RNA and terminate further chain extension, thus generating shorter products.
466 Assays for the evaluation of chain termination were usually non-competitive, in which
467 a nucleotide analog was present but its corresponding natural rNTP, either ATP, UTP,
468 GTP and CTP was absent, which forced the incorporation of the analog. In our
469 competitive assay, all 4 rNTPs were present. Therefore, the generation of fully
470 extended product was possible, even in the presence of a nucleotide analog. These
471 nucleotide analogs might have interfered the RNA extension by nsp12 without
472 incorporation. Or they could be removed from the RNA chain upon incorporation by
473 the pyrophosphorylation activity of nsp12 which had been clearly shown above. Both
474 could slow down the extension process and cause the decrease of product. The
475 competitive assay also resembled better the intracellular condition during drug
476 treatment in which all 4 rNTPs were present as well.

477

478 Based on the dose-response study of 2'-C-M-GTP, 4 mM was chosen as the screening
479 concentration for the 24 nucleotide analogs, except for emtricitabine which was
480 screened at 2 mM due to its low stock concentration. ATP, UTP, GTP and CTP at 4 mM

481 were used as controls. Their activities were averaged and defined as 100%. Relative
482 activity upon nucleotide analog treatment was normalized to the average and percent
483 of inhibition was calculated. **Figure 4B** showed the extended products by nsp12 upon
484 treatment with the 24 nucleotide analogs. **Figure 4C** showed the percent of inhibition
485 of the top 10 hits in the screening. Full list of inhibition by the 24 nucleotide analogs
486 was shown in **Table 1**. Compared to rNTPs control, 10 nucleotide analogs showed >40%
487 inhibition and 14 showed >20% inhibition including remdesivir, as shown by the
488 decrease of extended products. Interestingly, the two gemcitabine from different
489 suppliers showed identical levels of inhibition which suggested the screening assay
490 had high consistency. Of the 10 hits with >40% inhibition, 6 were anticancer drugs,
491 including clofarabine, 6-mercaptopurine, 8-oxo-GTP, 6-thio-GTP and the 2
492 gemcitabine, and 4 nucleotide analogs were antiviral drugs, including 2'-C-M-GTP,
493 stavudine, tenofovir and ganciclovir. All the 10 nucleotide analogs, except for 2'-C-M-
494 GTP and 8-oxo-GTP, were FDA-approved. And the 3 FDA-approved antiviral hits,
495 stavudine, tenofovir and ganciclovir, had acceptable safety profiles. Emtricitabine,
496 ribavirin and sofosbuvir, which are currently under evaluation for COVID-19 in clinical
497 trials, showed minimal inhibition against SARS-CoV nsp12. They either did not inhibit
498 nsp12 or required higher concentration to be effective. Or, they could have involved
499 other mechanisms to inhibit virus replication. This has been reported for ribavirin which
500 can inhibit virus replication by introducing mutations instead of inhibiting RNA/DNA
501 replication [102]. The effective concentration of ribavirin in cell culture could also be
502 high for some viruses [82, 103]. In addition, as compared to rNTP controls, the
503 pyrophosphorylation products of clofarabine and 2'-C-M-GTP were decreased while
504 most of the nucleotide analogs showed similar levels. As the top 2 hits, their higher
505 inhibition might have led to the decrease of pyrophosphorylation, or they might indicate
506 a different mechanism to inhibit RNA extension.

507

508 The top 10 hits were verified at 1, 2 and 4 mM, using the same assay as screening
509 (**Figure 5A**). All hits showed significant decrease of extension product in a dose-
510 dependent manner, except for ganciclovir which showed similar level of extension

511 product to ATP control at 4 mM. In addition, as an approved treatment for COVID-19,
512 remdesivir was also included in the verification assay which confirmed its inhibition on
513 nsp12 at 4 mM as observed in the screening. Inhibition on pyrophosphorylation for
514 clofarabine and 2'-C-M-GTP at 4 mM was also confirmed. Taken together, this study
515 supported the validity of the screening and confirmed all the hits in the screening,
516 except for ganciclovir, had obvious inhibition on nsp12.

517

518 **Discovery of stavudine and remdesivir as nsp12-specific antivirals**

519 As the competitive screening assay developed in this study was novel, we tried to
520 prove the validity of the assay from different perspectives. One good way is probably
521 to prove the hits in the screening were specific to nsp12. In **Figure 2B**, nsp8 was shown
522 to possess comparable RNA extension activity to nsp12, although it was tested at a
523 much higher concentration. Nsp8 had been proposed as a primase and certain
524 mutations in nsp8 region could lead to replication deficiency, even lethality, for SARS-
525 CoV [88]. Nsp8 was 3-fold smaller in size than nsp12 and lacked the seven
526 conservative motifs A to G, making nsp8 a reasonable control to identify nsp12-specific
527 drugs. We performed screening against nsp8 using the 24 nucleotide analogs (**Figure**
528 **5B**). The hits and their specificity to nsp12 were listed in **Table 1**. To our surprise, most
529 of the analogs in nsp8 screening showed similar patterns of inhibition to nsp12. This
530 result either suggested that the inhibition of RNA extension by these nucleotide
531 analogs was independent of nsp12 or nsp8, or suggested that nsp12 and nsp8 might
532 have evolved similar composition in the catalysis active site to better coordinate the
533 RNA replication for SARS-CoV. Interestingly, we did observe that the inhibition of
534 stavudine decreased by 20% from nsp12 to nsp8 and the inhibition of gemcitabine
535 increased by 30%, suggesting that stavudine had more specificity towards nsp12 while
536 gemcitabine had less. In addition, remdesivir, which had 28.44% inhibition against
537 nsp12, showed minimal inhibition against nsp8, suggesting that remdesivir was a
538 nsp12-specific drug completely. The specificity of stavudine and remdesivir to nsp12
539 did support the hits validity of the screening. To note, nsp12 is the major RdRp for
540 SARS-CoV and a specific drug may be favorable as they could improve efficacy and

541 reduce side effects. However, the efficacy can also be enhanced if a drug had dual
542 inhibition on nsp12 and nsp8. Therefore, the comparison between nsp12 and nsp8
543 screenings was only to prove the validity of the screening and not necessarily to be
544 able to identify a more potent hit.

545

546 **Stavudine, tenofovir, clofarabine and gemcitabine had inhibition on 2019-nCoV**
547 **nsp12**

548 Nsp12 was highly conservative among SARS-CoVs, inhibitors of SARS-CoV nsp12
549 most likely would inhibit 2019-nCoV as well. To confirm, we purified the nsp12 of 2019-
550 nCoV and evaluated its activity by the same single-stranded RNA primer used for
551 SARS-CoV. As shown by time-course study (**Figure 6A**), extended product could be
552 detected as early as 5 min and full activity was achieved at 120 min. This result
553 suggested that the nsp12 of 2019-nCoV could extend the RNA primer as efficiently as
554 SARS-CoV. Based on potency and safety, we then selected 4 of the 10 SARS-CoV
555 hits, stavudine, tenofovir, clofarabine and gemcitabine, in their corresponding
556 triphosphates, to be evaluated on 2019-nCoV nsp12 (**Figure 6B-C**). Ganciclovir and
557 remdesivir were also included. As compared to ATP control, stavudine, tenofovir,
558 clofarabine and gemcitabine showed significant decrease of extension products, while
559 ganciclovir and remdesivir showed low levels of decrease. This result suggested that
560 stavudine, tenofovir, clofarabine and gemcitabine could inhibit 2019-nCoV nsp12 as
561 well.

562

563 **Discovery of five HIV nucleoside analog reverse-transcriptase inhibitors (NRTIs)**
564 **with inhibition on nsp12**

565 HIV NRTIs had good safety profiles, making them ideal candidates for drug re-
566 purposing. In the screening, 3 HIV NRTIs were evaluated and 2 of them, stavudine
567 and tenofovir, showed inhibition on nsp12. It seemed HIV NRTIs had high possibility
568 to inhibit the nsp12 of SARS-CoVs, though the sample size was very small. To date, 8
569 NRTIs in total have been approved for HIV treatment. Five of them were not included
570 in the screening library due to commercial availability or delivery issues. We managed

571 to purchase all 8 NRTIs and tested them on nsp12 in their corresponding active
572 triphosphates. Clofarabine, an anticancer drug, was included as treatment control. A
573 primer control without nsp12 was also included. As shown by **Figure 7A**, in addition to
574 stavudine (44.64%) and tenofovir (43.23%), another 3 NRTIs, abacavir, zidovudine and
575 zalcitabine, were identified to be effective inhibitors against SARS-CoV nsp12, with
576 50.09%, 34.62%, and 89.67% inhibition, respectively (**Figure 7C**). The nsp12 of 2019-
577 nCoV showed identical results (**Figure 7B**), with 53.05%, 37.56% and 84.69%
578 inhibition for the 3 NRTIs, respectively (**Figure 7C**). The inhibition by zalcitabine was
579 almost complete at 4 mM. In addition, though not regarded as a hit, lamivudine also
580 showed low level of inhibition on both viruses (20.39% and 15.02%, respectively). To
581 verify the inhibition of the 3 newly identified NRTIs, they were evaluated at three
582 concentrations (1, 2 and 4 mM), with ATP and tenofovir used as controls (**Figure 8**).
583 The inhibition of all 3 NRTIs were confirmed at 4 mM and zalcitabine also showed
584 inhibition at 2 mM. Taken together, these results suggested that 5 HIV NRTIs, tenofovir,
585 stavudine, abacavir, zidovudine and zalcitabine, were effective inhibitors against the
586 nsp12 of both SARS-CoV and 2019-nCoV.

587

588 **Discussion**

589 **The dependence of nsp12 activity on K⁺ and divalent catalytic metals**

590 In this study, we expressed and purified active SARS-CoV nsp12 which could
591 efficiently extend a single-stranded RNA. The activity depended on K⁺ while Na⁺ led to
592 pyrophosphorylation and optimal activity was observed at concentrations close to the
593 physiological K⁺ concentration (140 to 150 mM) [101]. To our knowledge, this is the
594 first time such dependence had been reported for nsp12. Previously, nsp12 alone was
595 reported to be inactive [65, 88], which possibly could be explained by the conditions in
596 which the activities were determined, either with Na⁺ or low concentration of K⁺. In our
597 study, the activity of nsp12 was also dependent on Mg²⁺ or Mn²⁺, but due to its
598 intracellular predominance [93], Mg²⁺ should be the major catalytic metal for nsp12
599 physiologically. Interestingly, Mn²⁺ is mutagenetic and promotes mis-incorporation
600 during RNA synthesis. Viral RdRps in general had low replication fidelity and a relative

601 high mutation rate. Therefore, it is possible that nsp12 may take advantage of Mn^{2+} as
602 a cofactor to enhance mutation during replication by occasionally involving it into the
603 catalysis active site. Furthermore, our study proved that nsp12 alone could be fully
604 active at low concentration (16-32 nM) without the requirement of nsp7 and nsp8. The
605 full activity was only observed for single-stranded RNA, possibly via a back-priming
606 mechanism [88]. While for double-stranded RNA, the activity of nsp12 was very low
607 which was consistent with previous studies [58, 88]. As single-stranded RNA was
608 unstable, it may have intrinsic drive to back-prime and extend to form a stable double-
609 stranded structure. This intrinsic drive would promote the extension by nsp12 which
610 could explain the low activity of nsp12 observed for double-stranded RNA.

611

612 **Competitive assay for antiviral discovery against nsp12**

613 To discover nucleotide analogs against nsp12, a competitive assay was developed
614 which provided a rapid screening method to identify drugs with inhibition on nsp12.
615 Assays in previous studies were usually based on chain termination in which the
616 corresponding rNTP of a nucleotide analog, either ATP, UTP, CTP or GTP, was absent
617 to determine the efficiency of the analog to be incorporated into RNA chain and the
618 efficiency to cause chain termination. In contrast, we developed a competitive assay.
619 All the 4 rNTPs were present as well as a nucleotide analog. The nucleotide analog
620 would compete with its corresponding rNTP, which resembled the intracellular
621 condition during nucleotide analog treatment. Instead of showing chain termination
622 with shorter product, the assay showed decrease of the fully extended product. As a
623 catalyst, nsp12 could catalyze both RNA polymerization and the reverse process,
624 pyrophosphorylation. Therefore, it was highly possible that nsp12 could remove chain-
625 terminating nucleotide analogs from RNA chain upon incorporation, leading to the
626 absence of a terminated product. To our knowledge, this is the first time that nsp12 has
627 been shown to be associated with such property which provides a new perspective
628 about how nsp12 replicates SARS-CoVs genome intracellularly.

629

630

631 **High concentration for nsp12 antiviral screening**

632 In this study, we performed drug screening and identified 10 nucleotide analogs
633 with >40% and 14 with >20% inhibition on nsp12, including remdesivir, gemcitabine
634 and tenofovir. The screening concentration was 4 mM which was high. This should be
635 due to the short extension (7 bp) of the RNA product and high concentration of
636 nucleotide analogs had to be involved to show inhibition. SARS-CoVs have a genome
637 of 30 kbp and nucleotide analogs would be able to achieve similar levels of inhibition
638 at much lower concentrations intracellularly. Thus, further evaluation in cell culture is
639 necessary to better determine the effective concentrations of these analogs. But for
640 primary screening, this assay is sufficient for hits identification. In the screening,
641 remdesivir showed 28.44% inhibition on nsp12 and its effects has been proven in cell
642 cultures with $EC_{50} = 0.01 \mu\text{M}$ [104]. Another hit in our assay, gemcitabine, was also
643 reported to be able to inhibit SARS-CoV, MERS and 2019-nCoV at micromolar range
644 in cell culture [78, 79]. And recently, one study reported that tenofovir, in its tenofovir
645 disoproxil fumarate (TDF) form, inhibited 2019-nCoV at micromolar range in cell culture
646 [80]. In addition, a cohort study of HIV-positive persons receiving antiretroviral therapy
647 revealed that receiving TDF/FTC could lower the risk of 2019-nCoV hospitalization
648 [105]. These studies provide evidence that hits in our screening can inhibit SARS-CoVs
649 at micromolar range in cell culture.

650

651 **Drug-repurposing and combination of HIV NRTIs for COVID-19 treatment**

652 In this study, we identified 5 HIV NRTIs to be effective inhibitors against SARS-CoV
653 and 2019-nCoV. Among them, tenofovir, abacavir and zidovudine have superior safety
654 profiles than stavudine and zalcitabine [106, 107]. Zalcitabine has been discontinued
655 since 2006. Abacavir and stavudine share the same sugar backbone with a carbon-
656 carbon double bond. They probably can be used as an alternative to each other. But
657 as abacavir has a superior safety profile, it would be the first choice. Therefore,
658 tenofovir, abacavir and zidovudine are the top 3 hits we would like to propose as the
659 candidates to be further investigated for COVID-19 treatment. In addition, as proven
660 by antiretroviral therapies, drug combination is a powerful approach to improve therapy

661 efficacy and solve drug resistance issues. Therefore, we would also like to propose the
662 combinations of tenofovir, abacavir and zidovudine to be evaluated for COVID-19
663 treatment. During SARS outbreak, receiving highly active antiretroviral therapy
664 (HAART) was reported to be a protection factor against the virus [108]. In a recent
665 cohort study, taking tenofovir disoproxil fumarate (TDF) combined with emtricitabine
666 was associated with lower risk of 2019-nCoV hospitalization [105]. As emtricitabine
667 showed minimal inhibition on nsp12 in our study, the combination of tenofovir with
668 abacavir and/or zidovudine probably would have better efficacy against COVID-19, if
669 there is no antagonism among them. Lamivudine can also be included into the
670 combinations as it showed about 20% inhibition on nsp12 in our study. Currently, FDA-
671 approved HIV medicines combined by the 4 NRTIs include Epzicom
672 (abacavir/lamivudine), Trizivir (abacavir/lamivudine/zidovudine), Cimduo
673 (lamivudine/tenofovir disoproxil fumarate), and Combivir (lamivudine/zidovudine) [109].
674 Another choice for combination is type I interferons which can inhibit the replication of
675 2019-nCoV in cell culture [110] and have showed positive outcomes in clinical trials
676 [56, 111]. To conclude, we proposed 5 HIV NRTIs and their related combinations as
677 the candidates to be investigated for COVID-19 treatment. And we call for open
678 collaboration to get them further evaluated in cell cultures.

679

680 **Conclusion**

681 In this study, we expressed and purified active SARS-CoV nsp12 which could
682 efficiently extend single-stranded RNA in a K^+ and Mg^{2+} -dependent manner. We
683 developed a competitive assay for antiviral screening of nucleotide analogs against
684 nsp12 and identified 10 hits with more than 40% inhibition. We also discovered that
685 stavudine and remdesivir were specific antiviral to nsp12. In addition, 5 FDA-approved
686 HIV NRTIs, tenofovir, stavudine, abacavir, zidovudine and zalcitabine, were identified
687 to be effective inhibitors for the nsp12 of both SARS-CoV and 2019-nCoV. And we
688 proposed the 5 NRTIs and their related combinations to be further investigated as the
689 candidates for COVID-19 treatment.

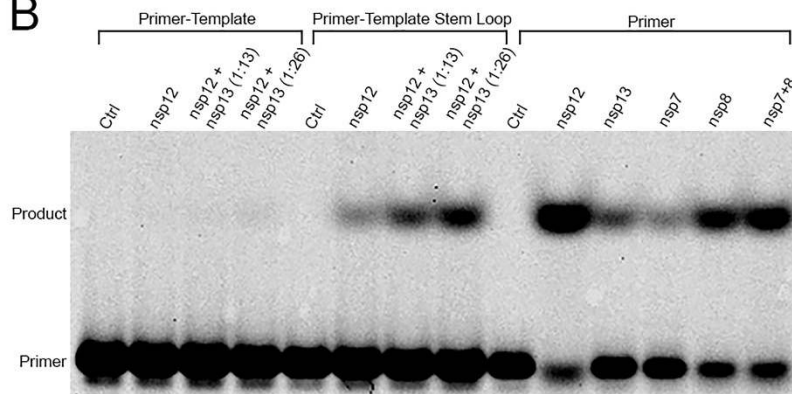
690

A

Primer: Cy5.5-5'-AACGUCUGUUCGCAAAAAGC-3'
 Template: 3'-UUGCAGACAAGCGUUUUUCGAGCUUAUUC-5'

Primer: Cy5.5-5'-AACGUCUGU ^{UCGC} AAAAAGC-3'
 Stem Loop: 3'-UUGCAGACA ^{UCGC} UUUUUCGUUCAGUUAUC-5'

B



C



711

712 **Figure 2 Back-priming extension activity of nsp12 on single-stranded RNA**

713 **primer. (A)** Two RNA templates were used in this study. One perfectly paired with the

714 Cy5.5-labeled RNA primer, which had been used in **Figure 1**. The other one formed a

715 stem-loop structure with the primer. The primer was annealed to template in a ratio of

716 1:3 to form a P/T complex. **(B)** The extension activity of nsp12 on the two primer-

717 template complexes was determined with combination of SARS-CoV helicase nsp13.

718 Two combination ratios were used: 1:13 and 1:26. The assay contained 25 mM Tris

719 HCl pH 8.0, 50 mM KCl, 1 mM DTT, 1 mM MgCl₂, 10 nM P/T complex, 16 nM nsp12,

720 210 or 420 nM nsp13, 100 μM rNTPs (25 μM each), 10% Glycerol, 6 mM NaCl and

721 0.02% triton X-100. The activities of nsp12, nsp13, nsp7 and nsp8 on the single-

722 stranded primer without a template were also determined. 50% Glycerol was used as

723 controls. Reaction mix was incubated at 37°C for 2h. **(C)** Back-priming mechanism was

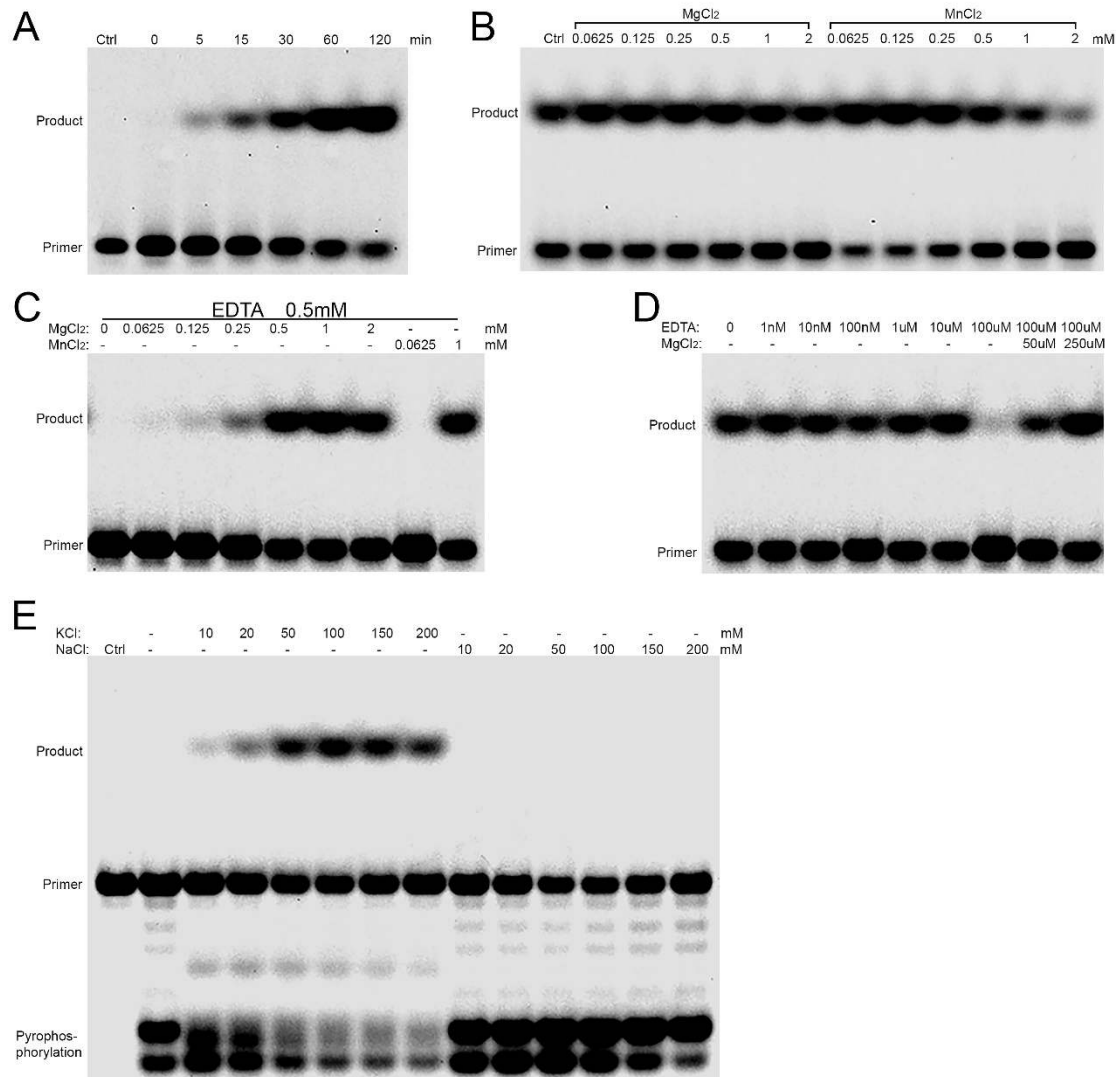
724 proposed. The sequence and secondary structure of the extended product was

725 predicted. Primer was shown in black and the extension was shown in red.

726

727

728

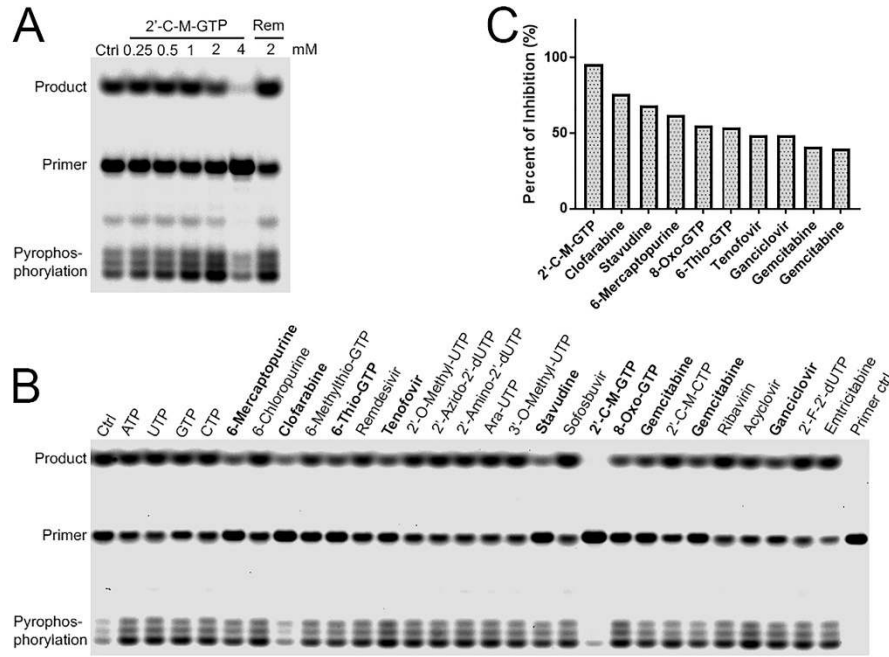


729

730 **Figure 3 The dependence of nsp12 activity on Mg²⁺ and K⁺.** (A) Time-course study
731 which showed the activity of nsp12 at various time-points towards the single-stranded
732 RNA primer without a template. The concentration of nsp12 and the RNA primer was
733 16 nM and 10 nM, respectively. (B) showed the activity of nsp12 on the primer under
734 various concentrations of Mg²⁺ or Mn²⁺, from 0.0625 to 2 mM. Control was added with
735 same volume of water. The assay indicated the presence of endogenous catalytic
736 metals, shown by the activity of control. (C) The assay was added with 0.5 mM EDTA
737 to block endogenous catalytic metals and the nsp12 activity under various
738 concentrations of Mg²⁺ or Mn²⁺ was re-determined. (D) The concentration of
739 endogenous catalytic metals was titrated by serially diluted EDTA. Water was used as
740 control. (E) Nsp12 activity was determined at various concentrations of K⁺ or Na⁺,
741 which showed that nsp12 was K⁺-dependent. Pyrophosphorylation activity was
742 observed for Na⁺. 50% Glycerol was used as enzymatic control. The concentration of
743 MgCl₂ in the assay was 1 mM.

744

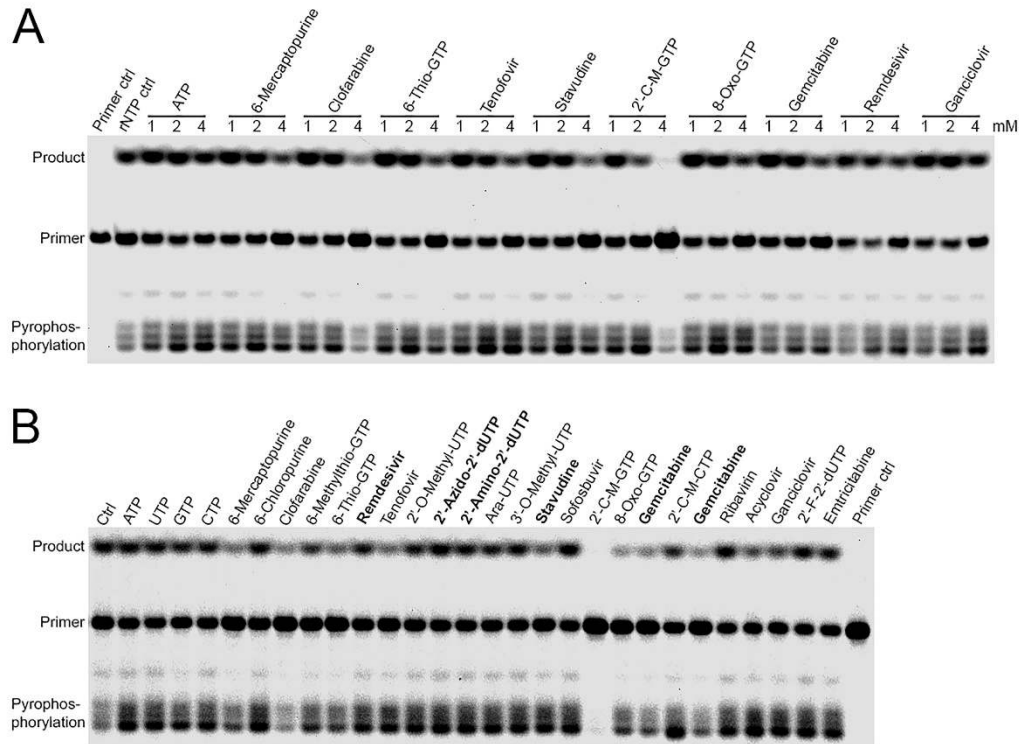
745



746

747 **Figure 4 Screening of 24 nucleotide analog triphosphates with inhibition on**
 748 **nsp12.** A competitive assay was developed which contained 16 nM nsp12, 10 nM RNA
 749 primer, 100 μ M rNTPs (25 μ M each) and a nucleotide analog in its corresponding
 750 triphosphate form. Reaction mix was incubated at 37°C for 30 min. An analog with
 751 inhibition on nsp12 would compete with a rNTP and decrease the amount of extended
 752 RNA product. **(A)** showed the dose-response of 2'-C-M-GTP and complete inhibition
 753 was observed at 4 mM which was used for the following screening concentration.
 754 Water was used as negative control. Remdesivir at 2 mM was also evaluated which
 755 showed no inhibition. **(B)** The inhibition of 24 nucleotide analogs in their corresponding
 756 triphosphate forms were screened at 4 mM using the competitive assay. Emtricitabine
 757 was screened at 2 mM due to low stock concentration. Same concentration of primer
 758 was loaded as negative control. 100 μ M rNTPs without adding extra nucleotide analog
 759 was also included as assay control. ATP, UTP, GTP and CTP at 4 mM was used as
 760 normalization controls and their activities were averaged and normalized to 100%.
 761 Relative percent of inhibition was calculated and hits with >40% inhibition were
 762 highlighted in bold. Inhibition on pyrophosphorylation was also observed for
 763 clofarabine and 2'-C-M-GTP. **(C)** showed percent of inhibition of the hits.

764

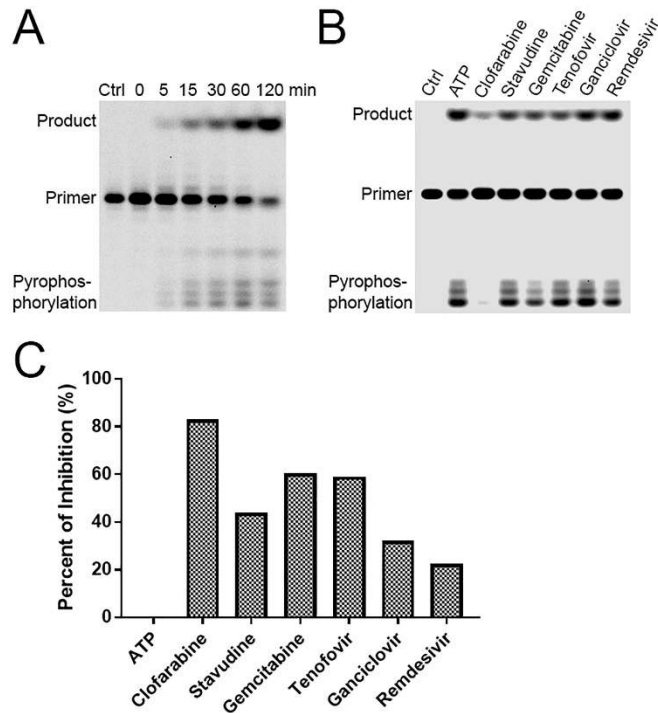


765

766 **Figure 5 Verification of nsp12 hits and the screening of nsp8.** (A) The nsp12 hits
 767 with >40% inhibition were verified at 1, 2, and 4 mM using the same assay as screening.
 768 Dose-dependent decrease of extended RNA product was observed. Remdesivir which
 769 had 28.44% inhibition on nsp12 was included as well. ATP was used as normalization
 770 control. Same concentration of primer was used as primer control. 100 μ M rNTPs
 771 without adding extra nucleotide was used as rNTP control. (B) The inhibition on nsp8
 772 of the 24 nucleotide analog triphosphates were also screened to identify nsp12-specific
 773 inhibitors and their inhibition percentages on nsp8 were compared to nsp12. Drugs
 774 with >20% differential inhibition between nsp12 and nsp8 were highlighted in bold.

775

776



777

778

779

780

781

782

783

784

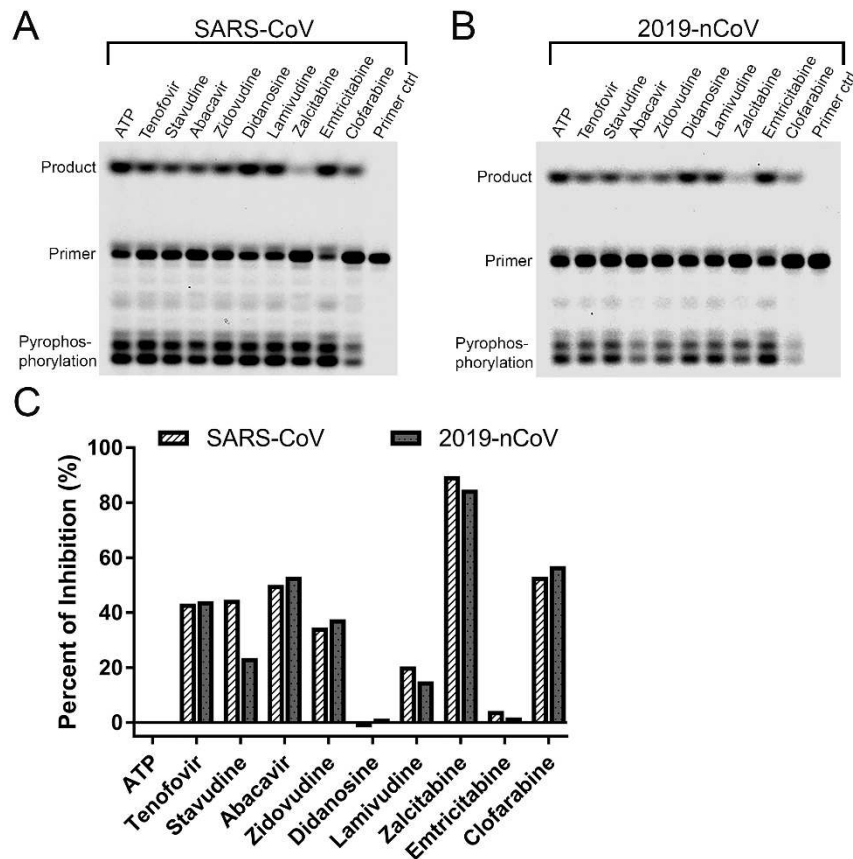
785

786

787

788

Figure 6 The inhibition of selected SARS-CoV hits on 2019-nCoV nsp12. (A) The activity of 2019-nCoV nsp12 was determined at different time-points which showed similar activities to SARS-CoV. 50% Glycerol incubated for 120 min was used as control. (B) Clofarabine, stavudine, gemcitabine, tenofovir, ganciclovir and remdesivir from SARS-CoV screening were selected and their inhibition on 2019-nCoV nsp12 was evaluated at 4 mM which showed inhibition as well. The assay condition was same as SARS-CoV. The analogs were evaluated in their corresponding triphosphate forms. ATP at 4 mM was used as normalization control. Same concentration of primer was loaded as negative control. (C) showed the percent of inhibition as compared to ATP of which the activity was defined as 100% and inhibition as zero.



789

790

791

792

793

794

795

796

797

798

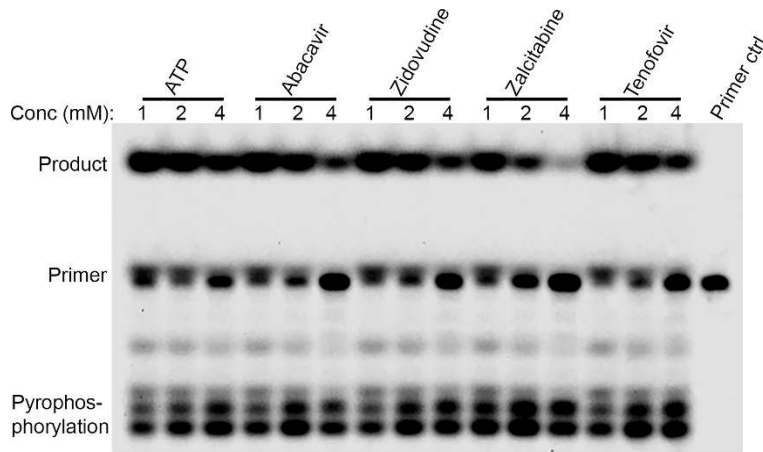
799

800

801

802

Figure 7 Drug-repurposing of HIV nucleoside analog reverse-transcriptase inhibitors (NRTIs) as antivirals against SARS-CoV and 2019-nCoV. Eight FDA-approved HIV NRTIs were evaluated for their inhibition on the nsp12 of SARS-CoV (**A**) and 2019-nCoV (**B**). The assay contained 16 nM nsp12, 10 nM RNA primer, 100 μ M rNTPs and 4 mM a NRTI, in its corresponding active triphosphate form. The extended product of the RNA primer by nsp12 upon NRTI treatment was analyzed by Urea-PAGE. Product was quantified and percent of inhibition was calculated. ATP was used as normalization control. Clofarabine, an anticancer drug, was used as treatment control. Assay with 50% glycerol instead of nsp12 was used as primer control. (**C**) showed the percent of inhibition of the 8 NRTIs, compared to ATP control. SARS-CoV was presented by white bar with slashes. 2019-nCoV was presented by gray bar with dots.



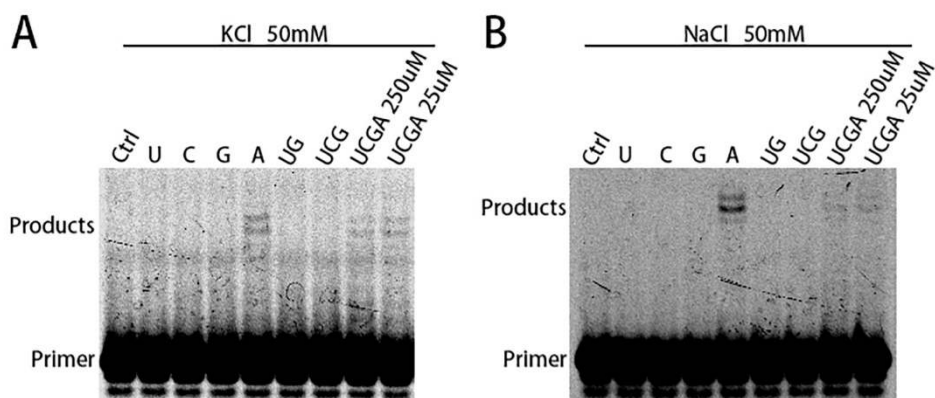
803

804 **Figure 8 Inhibition verification of abacavir, zidovudine and zalcitabine on nsp12.**

805 The three newly identified NRTIs, abacavir (carbovir-TP), zidovudine and zalcitabine
806 triphosphates, were verified at three concentrations (1, 2 and 4 mM) for their inhibition
807 on the RNA extension by nsp12, using SARS-CoV as a model. The Cy5.5-labeled RNA
808 primer was used and its extended product as well as pyrophosphorylation product by
809 SARS-CoV nsp12 were visualized. ATP was used as treatment negative control.
810 Tenofovir was used as treatment positive control. Reaction with 50% glycerol instead
811 of nsp12 was used as primer control. For abacavir and zidovudine, inhibition was
812 confirmed at 4 mM. For zalcitabine, inhibition was observed at both 2 and 4 mM.

813

814



815

816 **Figure S1 Poly A activity of nsp12 on double-stranded RNA.**

817 An RNA primer annealed to a template was used to determine the template-dependent poly A
818 activity of nsp12, with either single rNTP (UTP, CTP, GTP, ATP) or their combinations (UG,
819 UCG, UCGA). The concentration for each rNTP was 250 μ M. Water was used as
820 control and a control with 25 μ M each of UCGA was also included. The assay was
821 performed with 50 mM either KCl (A) or NaCl (B). ATP alone showed identical
822 extended products as UCGA while UTP, CTP, and GTP showed no extension, and the
823 extension length (9 nt) was close to the template. This study suggested nsp12 had
824 poly A activity.

825

826

Table 1. Inhibition of 24 nucleotide analogs on SARS-CoV nsp12 and nsp8.

Order	Nucleotide Analogs	Inhibition on Nsp12 (%)	Inhibition on Nsp8 (%)	Specificity to Nsp12 (%)
1	Primer control	100.00	100.00	0.00
2	2'-C-M-GTP	95.94	98.63	-2.69
3	Clofarabine-TP	75.84	62.27	13.57
4	Stavudine-TP	68.16	44.60	23.56
5	6-Mercaptopurine-TP	62.05	59.94	2.11
6	8-Oxo-GTP	55.38	69.45	-14.07
7	6-Thio-GTP	53.77	53.62	0.15
8	Tenofovir-DP	48.94	47.24	1.71
9	Ganciclovir-TP	48.94	33.74	15.20
10	Gemcitabine-TP	40.90	73.56	-32.65
11	Gemcitabine-TP	40.10	70.43	-30.33
12	6-Methylthio-GTP	30.85	23.31	7.54
13	Remdesivir-DP	28.44	1.23	27.22
14	Acyclovir-TP	26.03	35.58	-9.55
15	2'-O-methyl-UTP	21.21	9.20	12.00
16	2'-Amino-2'-dUTP	14.37	-9.20	23.57
17	2'-Azido-2'-dUTP	10.35	-12.88	23.24
18	Emtricitabine-TP	10.35	15.34	-4.99
19	ATP	7.54	-4.91	12.45
20	2'-C-M-CTP	5.53	22.09	-16.56
21	2'-F-2'-dUTP	5.13	-2.45	7.58
22	Ara-UTP	4.72	21.47	-16.75
23	CTP	1.51	-4.29	5.80
24	3'-O-methyl-UTP	-0.10	-1.23	1.13
25	GTP	-0.90	13.50	-14.40
26	6-Chloropurine-TP	-2.91	-15.34	12.42
27	100 μ M rNTP ctrl	-7.34	-15.34	8.00
28	UTP	-8.14	-5.52	-2.62
29	Ribavirin-TP	-24.62	-12.88	-11.74
30	Sofosbuvir-DP	-27.44	-21.47	-5.96

827

828 Reference

- 829 1. Wu, A., et al., *Genome Composition and Divergence of the Novel Coronavirus (2019-*
830 *nCoV) Originating in China*. Cell Host Microbe, 2020. **27**(3): p. 325-328.
- 831 2. Brian, D.A. and R.S. Baric, *Coronavirus genome structure and replication*. Curr Top
832 Microbiol Immunol, 2005. **287**: p. 1-30.
- 833 3. Li, W., et al., *Animal origins of the severe acute respiratory syndrome coronavirus: insight*
834 *from ACE2-S-protein interactions*. J Virol, 2006. **80**(9): p. 4211-9.
- 835 4. Hu, B., et al., *Discovery of a rich gene pool of bat SARS-related coronaviruses provides*
836 *new insights into the origin of SARS coronavirus*. PLoS Pathog, 2017. **13**(11): p. e1006698.

- 837 5. Zhou, P., et al., *A pneumonia outbreak associated with a new coronavirus of probable bat*
838 *origin*. Nature, 2020. **579**(7798): p. 270-273.
- 839 6. Zhang, T., Q. Wu, and Z. Zhang, *Probable Pangolin Origin of SARS-CoV-2 Associated with*
840 *the COVID-19 Outbreak*. Curr Biol, 2020. **30**(8): p. 1578.
- 841 7. Liu, P., et al., *Are pangolins the intermediate host of the 2019 novel coronavirus (SARS-*
842 *CoV-2)?* PLoS Pathog, 2020. **16**(5): p. e1008421.
- 843 8. Zhao, X., et al., *Broad and Differential Animal Angiotensin-Converting Enzyme 2 Receptor*
844 *Usage by SARS-CoV-2*. J Virol, 2020. **94**(18).
- 845 9. Lam, S.D., et al., *SARS-CoV-2 spike protein predicted to form complexes with host*
846 *receptor protein orthologues from a broad range of mammals*. Sci Rep, 2020. **10**(1): p.
847 16471.
- 848 10. Chen, Y., et al., *Rhesus angiotensin converting enzyme 2 supports entry of severe acute*
849 *respiratory syndrome coronavirus in Chinese macaques*. Virology, 2008. **381**(1): p. 89-97.
- 850 11. Matyasek, R. and A. Kovarik, *Mutation Patterns of Human SARS-CoV-2 and Bat RaTG13*
851 *Coronavirus Genomes Are Strongly Biased Towards C>U Transitions, Indicating Rapid*
852 *Evolution in Their Hosts*. Genes (Basel), 2020. **11**(7).
- 853 12. Li, Y.Y., X.; Wang, N.; Wang, H.; Yin, B.; Yang, X.; Jiang, W., *The divergence between SARS-*
854 *CoV-2 and RaTG13 might be overestimated due to the extensive RNA modification*.
855 Future Virol, 2020.
- 856 13. Di Giorgio, S., et al., *Evidence for host-dependent RNA editing in the transcriptome of*
857 *SARS-CoV-2*. Sci Adv, 2020. **6**(25): p. eabb5813.
- 858 14. Andersen, K.G., et al., *The proximal origin of SARS-CoV-2*. Nat Med, 2020. **26**(4): p. 450-
859 452.
- 860 15. Wrobel, A.G., et al., *SARS-CoV-2 and bat RaTG13 spike glycoprotein structures inform on*
861 *virus evolution and furin-cleavage effects*. Nat Struct Mol Biol, 2020. **27**(8): p. 763-767.
- 862 16. Hoffmann, M., H. Kleine-Weber, and S. Pohlmann, *A Multibasic Cleavage Site in the Spike*
863 *Protein of SARS-CoV-2 Is Essential for Infection of Human Lung Cells*. Mol Cell, 2020.
864 **78**(4): p. 779-784 e5.
- 865 17. Walls, A.C., et al., *Structure, Function, and Antigenicity of the SARS-CoV-2 Spike*
866 *Glycoprotein*. Cell, 2020. **181**(2): p. 281-292 e6.
- 867 18. Li, X., et al., *Emergence of SARS-CoV-2 through recombination and strong purifying*
868 *selection*. Sci Adv, 2020. **6**(27).
- 869 19. Lv, L.L., G.; Chen, J.; Liang, X.; Li, Y., *Comparative genomic analysis revealed specific*
870 *mutation pattern between human coronavirus SARS-CoV-2 and Bat-SARSr-CoV RaTG13*.
871 bioRxiv, 2020.
- 872 20. Shang, J., et al., *Structural basis of receptor recognition by SARS-CoV-2*. Nature, 2020.
873 **581**(7807): p. 221-224.
- 874 21. Wrapp, D., et al., *Cryo-EM structure of the 2019-nCoV spike in the prefusion*
875 *conformation*. Science, 2020. **367**(6483): p. 1260-1263.
- 876 22. Li, F., et al., *Structure of SARS coronavirus spike receptor-binding domain complexed with*
877 *receptor*. Science, 2005. **309**(5742): p. 1864-8.
- 878 23. Lan, J., et al., *Structure of the SARS-CoV-2 spike receptor-binding domain bound to the*
879 *ACE2 receptor*. Nature, 2020. **581**(7807): p. 215-220.
- 880 24. Bosch, B.J., et al., *The coronavirus spike protein is a class I virus fusion protein: structural*

- 881 *and functional characterization of the fusion core complex.* J Virol, 2003. **77**(16): p. 8801-
882 11.
- 883 25. Traggiai, E., et al., *An efficient method to make human monoclonal antibodies from*
884 *memory B cells: potent neutralization of SARS coronavirus.* Nat Med, 2004. **10**(8): p. 871-
885 5.
- 886 26. Pinto, D., et al., *Cross-neutralization of SARS-CoV-2 by a human monoclonal SARS-CoV*
887 *antibody.* Nature, 2020. **583**(7815): p. 290-295.
- 888 27. Wang, C., et al., *A human monoclonal antibody blocking SARS-CoV-2 infection.* Nat
889 Commun, 2020. **11**(1): p. 2251.
- 890 28. Ju, B., et al., *Human neutralizing antibodies elicited by SARS-CoV-2 infection.* Nature,
891 2020. **584**(7819): p. 115-119.
- 892 29. Baum, A., et al., *Antibody cocktail to SARS-CoV-2 spike protein prevents rapid mutational*
893 *escape seen with individual antibodies.* Science, 2020. **369**(6506): p. 1014-1018.
- 894 30. Zost, S.J., et al., *Potently neutralizing and protective human antibodies against SARS-CoV-*
895 *2.* Nature, 2020. **584**(7821): p. 443-449.
- 896 31. Wong, S.K., et al., *A 193-amino acid fragment of the SARS coronavirus S protein efficiently*
897 *binds angiotensin-converting enzyme 2.* J Biol Chem, 2004. **279**(5): p. 3197-201.
- 898 32. Du, L., et al., *The spike protein of SARS-CoV--a target for vaccine and therapeutic*
899 *development.* Nat Rev Microbiol, 2009. **7**(3): p. 226-36.
- 900 33. Salvatori, G., et al., *SARS-CoV-2 SPIKE PROTEIN: an optimal immunological target for*
901 *vaccines.* J Transl Med, 2020. **18**(1): p. 222.
- 902 34. Barnes, C.O., et al., *Structures of Human Antibodies Bound to SARS-CoV-2 Spike Reveal*
903 *Common Epitopes and Recurrent Features of Antibodies.* Cell, 2020. **182**(4): p. 828-842
904 e16.
- 905 35. Zhang, J., et al., *Progress and Prospects on Vaccine Development against SARS-CoV-2.*
906 Vaccines (Basel), 2020. **8**(2).
- 907 36. He, Y., et al., *Receptor-binding domain of SARS-CoV spike protein induces highly potent*
908 *neutralizing antibodies: implication for developing subunit vaccine.* Biochem Biophys Res
909 Commun, 2004. **324**(2): p. 773-81.
- 910 37. COVID-19 VACCINE TRACKER, 2020. <https://www.covid-19vaccinetracker.org/>.
- 911 38. Du, Q.S., et al., *Polyprotein cleavage mechanism of SARS CoV Mpro and chemical*
912 *modification of the octapeptide.* Peptides, 2004. **25**(11): p. 1857-64.
- 913 39. Ullrich, S. and C. Nitsche, *The SARS-CoV-2 main protease as drug target.* Bioorg Med
914 Chem Lett, 2020. **30**(17): p. 127377.
- 915 40. Xue, X., et al., *Structures of two coronavirus main proteases: implications for substrate*
916 *binding and antiviral drug design.* J Virol, 2008. **82**(5): p. 2515-27.
- 917 41. Zhang, L., et al., *Crystal structure of SARS-CoV-2 main protease provides a basis for*
918 *design of improved alpha-ketoamide inhibitors.* Science, 2020. **368**(6489): p. 409-412.
- 919 42. Douangamath, A., et al., *Crystallographic and electrophilic fragment screening of the*
920 *SARS-CoV-2 main protease.* Nat Commun, 2020. **11**(1): p. 5047.
- 921 43. Yang, H., et al., *The crystal structures of severe acute respiratory syndrome virus main*
922 *protease and its complex with an inhibitor.* Proc Natl Acad Sci U S A, 2003. **100**(23): p.
923 13190-5.
- 924 44. Hegyi, A. and J. Ziebuhr, *Conservation of substrate specificities among coronavirus main*

- 925 *proteases*. J Gen Virol, 2002. **83**(Pt 3): p. 595-599.
- 926 45. Wang, J., *Fast Identification of Possible Drug Treatment of Coronavirus Disease-19*
927 *(COVID-19) through Computational Drug Repurposing Study*. J Chem Inf Model, 2020.
928 **60**(6): p. 3277-3286.
- 929 46. Kandeel, M. and M. Al-Nazawi, *Virtual screening and repurposing of FDA approved drugs*
930 *against COVID-19 main protease*. Life Sci, 2020. **251**: p. 117627.
- 931 47. Arya, R.D., A.; Prashar, V.; Kumar, M., *Potential inhibitors against papain-like protease of*
932 *novel coronavirus (SARS-CoV-2) from FDA approved drugs*. ChemRxiv, 2020.
- 933 48. Das, S., et al., *An investigation into the identification of potential inhibitors of SARS-CoV-*
934 *2 main protease using molecular docking study*. J Biomol Struct Dyn, 2020: p. 1-11.
- 935 49. Khan, R.J., et al., *Targeting SARS-CoV-2: a systematic drug repurposing approach to*
936 *identify promising inhibitors against 3C-like proteinase and 2'-O-ribose*
937 *methyltransferase*. J Biomol Struct Dyn, 2020: p. 1-14.
- 938 50. Muralidharan, N., et al., *Computational studies of drug repurposing and synergism of*
939 *lopinavir, oseltamivir and ritonavir binding with SARS-CoV-2 protease against COVID-19*.
940 J Biomol Struct Dyn, 2020: p. 1-6.
- 941 51. Pillaiyar, T., et al., *An Overview of Severe Acute Respiratory Syndrome-Coronavirus*
942 *(SARS-CoV) 3CL Protease Inhibitors: Peptidomimetics and Small Molecule Chemotherapy*.
943 J Med Chem, 2016. **59**(14): p. 6595-628.
- 944 52. Cao, B., et al., *A Trial of Lopinavir-Ritonavir in Adults Hospitalized with Severe Covid-19*.
945 N Engl J Med, 2020. **382**(19): p. 1787-1799.
- 946 53. Horby, P.W., et al., *Lopinavir-ritonavir in patients admitted to hospital with COVID-19*
947 *(RECOVERY): a randomised, controlled, open-label, platform trial*. The Lancet, 2020.
- 948 54. Osborne, V., et al., *Lopinavir-Ritonavir in the Treatment of COVID-19: A Dynamic*
949 *Systematic Benefit-Risk Assessment*. Drug Saf, 2020. **43**(8): p. 809-821.
- 950 55. Zhu, Z., et al., *Arbidol monotherapy is superior to lopinavir/ritonavir in treating COVID-*
951 *19*. J Infect, 2020. **81**(1): p. e21-e23.
- 952 56. Hung, I.F., et al., *Triple combination of interferon beta-1b, lopinavir-ritonavir, and ribavirin*
953 *in the treatment of patients admitted to hospital with COVID-19: an open-label,*
954 *randomised, phase 2 trial*. Lancet, 2020. **395**(10238): p. 1695-1704.
- 955 57. Stower, H., *Lopinavir-ritonavir in severe COVID-19*. Nat Med, 2020. **26**(4): p. 465.
- 956 58. Ahn, D.G., et al., *Biochemical characterization of a recombinant SARS coronavirus nsp12*
957 *RNA-dependent RNA polymerase capable of copying viral RNA templates*. Arch Virol,
958 2012. **157**(11): p. 2095-104.
- 959 59. te Velthuis, A.J., et al., *The RNA polymerase activity of SARS-coronavirus nsp12 is primer*
960 *dependent*. Nucleic Acids Res, 2010. **38**(1): p. 203-14.
- 961 60. te Velthuis, A.J., S.H. van den Worm, and E.J. Snijder, *The SARS-coronavirus nsp7+nsp8*
962 *complex is a unique multimeric RNA polymerase capable of both de novo initiation and*
963 *primer extension*. Nucleic Acids Res, 2012. **40**(4): p. 1737-47.
- 964 61. Imbert, I., et al., *A second, non-canonical RNA-dependent RNA polymerase in SARS*
965 *coronavirus*. EMBO J, 2006. **25**(20): p. 4933-42.
- 966 62. Kirchdoerfer, R.N. and A.B. Ward, *Structure of the SARS-CoV nsp12 polymerase bound to*
967 *nsp7 and nsp8 co-factors*. Nat Commun, 2019. **10**(1): p. 2342.
- 968 63. Hillen, H.S., et al., *Structure of replicating SARS-CoV-2 polymerase*. Nature, 2020.

- 969 **584**(7819): p. 154-156.
- 970 64. Bruenn, J.A., *A structural and primary sequence comparison of the viral RNA-dependent*
971 *RNA polymerases*. Nucleic Acids Res, 2003. **31**(7): p. 1821-9.
- 972 65. Wang, Q., et al., *Structural Basis for RNA Replication by the SARS-CoV-2 Polymerase*. Cell,
973 2020. **182**(2): p. 417-428 e13.
- 974 66. Lehmann, K.C., et al., *Discovery of an essential nucleotidylating activity associated with a*
975 *newly delineated conserved domain in the RNA polymerase-containing protein of all*
976 *nidoviruses*. Nucleic Acids Res, 2015. **43**(17): p. 8416-34.
- 977 67. Wu, C., et al., *Analysis of therapeutic targets for SARS-CoV-2 and discovery of potential*
978 *drugs by computational methods*. Acta Pharm Sin B, 2020. **10**(5): p. 766-788.
- 979 68. Wang, Y., et al., *RNA-dependent RNA polymerase of SARS-CoV-2 as a therapeutic target*.
980 J Med Virol, 2020.
- 981 69. Ruan, Z., et al., *SARS-CoV-2 and SARS-CoV: Virtual screening of potential inhibitors*
982 *targeting RNA-dependent RNA polymerase activity (NSP12)*. J Med Virol, 2020.
- 983 70. Mutlu, O., et al., *Targeting SARS-CoV-2 Nsp12/Nsp8 interaction interface with approved*
984 *and investigational drugs: an in silico structure-based approach*. J Biomol Struct Dyn, 2020:
985 p. 1-13.
- 986 71. Elfiky, A.A., *Ribavirin, Remdesivir, Sofosbuvir, Galidesivir, and Tenofovir against SARS-*
987 *CoV-2 RNA dependent RNA polymerase (RdRp): A molecular docking study*. Life Sci, 2020.
988 **253**: p. 117592.
- 989 72. Ju, J., et al., *Nucleotide Analogues as Inhibitors of Viral Polymerases*. bioRxiv, 2020.
- 990 73. Jacome, R., et al., *Sofosbuvir as a potential alternative to treat the SARS-CoV-2 epidemic*.
991 Sci Rep, 2020. **10**(1): p. 9294.
- 992 74. Chien, M., et al., *Nucleotide Analogues as Inhibitors of SARS-CoV-2 Polymerase*. bioRxiv,
993 2020.
- 994 75. Chien, M., et al., *Nucleotide Analogues as Inhibitors of SARS-CoV-2 Polymerase, a Key*
995 *Drug Target for COVID-19*. J Proteome Res, 2020.
- 996 76. Jockusch, S., et al., *Triphosphates of the Two Components in DESCOVY and TRUVADA are*
997 *Inhibitors of the SARS-CoV-2 Polymerase*. bioRxiv, 2020.
- 998 77. Jockusch, S., et al., *A library of nucleotide analogues terminate RNA synthesis catalyzed*
999 *by polymerases of coronaviruses that cause SARS and COVID-19*. Antiviral Res, 2020. **180**:
1000 p. 104857.
- 1001 78. Dyall, J., et al., *Repurposing of clinically developed drugs for treatment of Middle East*
1002 *respiratory syndrome coronavirus infection*. Antimicrob Agents Chemother, 2014. **58**(8):
1003 p. 4885-93.
- 1004 79. Zhang, Y.N., et al., *Gemcitabine, lycorine and oxysophoridine inhibit novel coronavirus*
1005 *(SARS-CoV-2) in cell culture*. Emerg Microbes Infect, 2020. **9**(1): p. 1170-1173.
- 1006 80. Clososki, G., et al., *Tenofovir Disoproxil Fumarate: New Chemical Developments and*
1007 *Encouraging in vitro Biological Results for SARS-CoV-2*. Journal of the Brazilian Chemical
1008 Society, 2020.
- 1009 81. Park, S.J., et al., *Antiviral Efficacies of FDA-Approved Drugs against SARS-CoV-2 Infection*
1010 *in Ferrets*. mBio, 2020. **11**(3).
- 1011 82. Morgenstern, B., et al., *Ribavirin and interferon-beta synergistically inhibit SARS-*
1012 *associated coronavirus replication in animal and human cell lines*. Biochem Biophys Res

- 1013 Commun, 2005. **326**(4): p. 905-8.
- 1014 83. Khalili, J.S., et al., *Novel coronavirus treatment with ribavirin: Groundwork for an evaluation*
1015 *concerning COVID-19*. J Med Virol, 2020. **92**(7): p. 740-746.
- 1016 84. Beigel, J.H., et al., *Remdesivir for the Treatment of Covid-19 - Final Report*. N Engl J Med,
1017 2020.
- 1018 85. Lu, G., et al., *Analysis of Ribonucleotide 5'-Triphosphate Analogs as Potential Inhibitors of*
1019 *Zika Virus RNA-Dependent RNA Polymerase by Using Nonradioactive Polymerase Assays*.
1020 Antimicrob Agents Chemother, 2017. **61**(3).
- 1021 86. Lin, Z. and H.S. Rye, *GroEL-mediated protein folding: making the impossible, possible*.
1022 Crit Rev Biochem Mol Biol, 2006. **41**(4): p. 211-39.
- 1023 87. Svetlov, V. and E. Nudler, *Basic mechanism of transcription by RNA polymerase II*. Biochim
1024 Biophys Acta, 2013. **1829**(1): p. 20-8.
- 1025 88. Subissi, L., et al., *One severe acute respiratory syndrome coronavirus protein complex*
1026 *integrates processive RNA polymerase and exonuclease activities*. Proc Natl Acad Sci U S
1027 A, 2014. **111**(37): p. E3900-9.
- 1028 89. Chen, J., et al., *Structural Basis for Helicase-Polymerase Coupling in the SARS-CoV-2*
1029 *Replication-Transcription Complex*. Cell, 2020. **182**(6): p. 1560-1573 e13.
- 1030 90. Adedeji, A.O., et al., *Mechanism of nucleic acid unwinding by SARS-CoV helicase*. PLoS
1031 One, 2012. **7**(5): p. e36521.
- 1032 91. von Brunn, A., et al., *Analysis of intraviral protein-protein interactions of the SARS*
1033 *coronavirus ORFome*. PLoS One, 2007. **2**(5): p. e459.
- 1034 92. Konkolova, E., et al., *Structural analysis of the putative SARS-CoV-2 primase complex*. J
1035 Struct Biol, 2020. **211**(2): p. 107548.
- 1036 93. Romani, A.M., *Cellular magnesium homeostasis*. Arch Biochem Biophys, 2011. **512**(1): p.
1037 1-23.
- 1038 94. Kumar, K.K., et al., *Cellular manganese content is developmentally regulated in human*
1039 *dopaminergic neurons*. Sci Rep, 2014. **4**: p. 6801.
- 1040 95. Tholey, G., et al., *Concentrations of physiologically important metal ions in glial cells*
1041 *cultured from chick cerebral cortex*. Neurochem Res, 1988. **13**(1): p. 45-50.
- 1042 96. Klenow, H. and I. Henningsen, *Effect of monovalent cations on the activity of the DNA*
1043 *polymerase of Escherichia coli B*. Eur J Biochem, 1969. **9**(1): p. 133-41.
- 1044 97. Savochkina, L.P. and R. Bibilashvili, *[Influence of ionic strength on RNA-polymerase*
1045 *structure]*. Mol Biol (Mosk), 1979. **13**(3): p. 509-18.
- 1046 98. Shiman, R. and D.E. Draper, *Stabilization of RNA tertiary structure by monovalent cations*.
1047 J Mol Biol, 2000. **302**(1): p. 79-91.
- 1048 99. Vieregg, J., et al., *Measurement of the effect of monovalent cations on RNA hairpin*
1049 *stability*. J Am Chem Soc, 2007. **129**(48): p. 14966-73.
- 1050 100. Lambert, D., et al., *The influence of monovalent cation size on the stability of RNA tertiary*
1051 *structures*. J Mol Biol, 2009. **390**(4): p. 791-804.
- 1052 101. Thier, S.O., *Potassium physiology*. Am J Med, 1986. **80**(4A): p. 3-7.
- 1053 102. Mejer, N., et al., *Ribavirin-induced mutagenesis across the complete open reading frame*
1054 *of hepatitis C virus genotypes 1a and 3a*. J Gen Virol, 2018. **99**(8): p. 1066-1077.
- 1055 103. Zhang, G., et al., *In vitro and in vivo evaluation of ribavirin and pleconaril antiviral activity*
1056 *against enterovirus 71 infection*. Arch Virol, 2012. **157**(4): p. 669-79.

- 1057 104. Pruijssers, A.J., et al., *Remdesivir Inhibits SARS-CoV-2 in Human Lung Cells and Chimeric*
1058 *SARS-CoV Expressing the SARS-CoV-2 RNA Polymerase in Mice*. Cell Rep, 2020. **32**(3): p.
1059 107940.
- 1060 105. Del Amo, J., et al., *Incidence and Severity of COVID-19 in HIV-Positive Persons Receiving*
1061 *Antiretroviral Therapy : A Cohort Study*. Ann Intern Med, 2020. **173**(7): p. 536-541.
- 1062 106. Margolis, A.M., et al., *A review of the toxicity of HIV medications*. J Med Toxicol, 2014.
1063 **10**(1): p. 26-39.
- 1064 107. Holec, A.D., et al., *Nucleotide Reverse Transcriptase Inhibitors: A Thorough Review,*
1065 *Present Status and Future Perspective as HIV Therapeutics*. Curr HIV Res, 2017. **15**(6): p.
1066 411-421.
- 1067 108. Chen, X.P. and Y. Cao, *Consideration of highly active antiretroviral therapy in the*
1068 *prevention and treatment of severe acute respiratory syndrome*. Clin Infect Dis, 2004.
1069 **38**(7): p. 1030-2.
- 1070 109. *FDA-Approved HIV Medicines*. HIVinfo.NIH.gov, 2020.
1071 <https://hivinfo.nih.gov/understanding-hiv/fact-sheets/fda-approved-hiv->
1072 [medicines](https://hivinfo.nih.gov/understanding-hiv/fact-sheets/fda-approved-hiv-).
- 1073 110. Mantlo, E., et al., *Antiviral activities of type I interferons to SARS-CoV-2 infection*. Antiviral
1074 Res, 2020. **179**: p. 104811.
- 1075 111. Sallard, E., et al., *Type 1 interferons as a potential treatment against COVID-19*. Antiviral
1076 Res, 2020. **178**: p. 104791.
- 1077